ROLL RESONANCE AND LOCK-IN OF FINNED PROJECTILES

By

ANANTHKRISHNAN NARAYAN

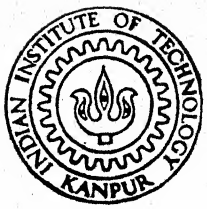

DEPARTMENT OF AEROSPACE ENGINEERING

INDIAN INSTITUTE OF TECHNOLOGY KANPUR - 208016

NOVEMBER, 1990

ROLL RESONANCE AND LOCK-IN OF FINNED PROJECTILES

A Thesis Submitted
in Partial Fulfilment of the Requirements
for the Degree of
MASTER OF TECHNOLOGY

By
ANANTHKRISHNAN NARAYAN

to the

DEPARTMENT OF AEROSPACE ENGINEERING
INDIAN INSTITUTE OF TECHNOLOGY KANPUR
NOVEMBER, 1990

AE-1990-M-NAR-ROLL

CERTIFICATE

It is certified that the work contained in the thesis entitled "ROLL RESONANCE AND LOCK-IN OF FINNED PROJECTILES", by Ananthkrishnan Narayan, has been carried out under our supervision and that this work has not been submitted elsewhere for a degree.

S.C.RAISINGHANI
Professor
Department of Aerospace Engineering

S.PRADEEP
Asst. Professor
Department of Aerospace Engineering

I.I.T. Kanpur

November, 1990

ABSTRACT

The problem of roll lock-in has gained importance with the use of finned projectiles as anti-tank ammunition. We consider a slightly asymmetric projectile with a trim angle that rotates with the projectile and shows large amplification when the projectile roll rate resonates with its nutation frequency. For a projectile with an offset center-of-mass, the trim angle induces a roll moment which can cause the roll rate to lock in at resonance.

The present study considers lock-in solutions obtained for different combinations of parameters of the nonlinear system for the projectile angular motion. Both normal lock-in, where the spin is in the same sense as the expected steady-state spin, and reverse lock-in, where the spin is in the opposite sense, are shown. Stability of these lock-in solutions and the influence of initial conditions on the steady-state response are studied. Stable lock-in is seen to occur only for a small fraction of the initial conditions tested. This is shown to be due to the presence of an unstable equilibrium near a stable lock-in solution.

Other anomalous roll behavior of rolling finned projectiles like transient resonance, catastrophic yaw, and roll break-out are also studied. The present analysis reveals that a projectile at transient resonance shows increased damping in yaw, contrary to the expected yaw build-up due to resonance. It is shown that catastrophic yaw can be explained without introducing nonlinear side moments in the analysis. Furthermore, it is shown that lock-in can occur even when the equilibrium at resonance is known to be unstable.

ACKNOWLEDGEMENT

I would like to express my sincere gratitude to Dr.S.C.Raisinghani and Dr.S.Pradeep for their constant encouragement, unwavering enthusiasm, and whole-hearted co-operation, and for the confidence that they reposed in me.

Thanks are due Mr.A.K.Ghosh, Scientist, ARDE, Pune, from whom I have learnt much and but for whom this thesis would never have seen the light of day.

I must also acknowledge the help rendered by my friends, Giresh K. Singh, Ranjit D. Pradhan, Manoj S. Medhekar, Vijay A. Pankhawala, Nachiketa Tiwari, Raman Pal Singh, P. Tarakeshwar, Shankha Pal, Makarand G. Joshi, and Rajiv Tiwari. I am deeply obliged to all of them.

Ananthkrishnan Narayan

TABLE OF CONTENTS

Chapter			Page
	LIST OF FIGURES		vi
	LIST OF TABLES		vii
	LIST OF SYMBOLS		viii
I	INTRODUCTION		1
II	LINEAR THEORY		
	2.1	Aeroballistic Axes	6
	2.2	Equations of Motion	6
	2.3	Tricyclic Motion	9
	2.4	Resonance	11
III	LOCK-IN THEORY		
	3.1	Roll Equation	16
	3.2	Center-of-Mass Offset	17
	3.3	Equilibrium Solutions	19
	3.4	Lock-in Stability	23
IV	RESULTS AND DISCUSSION		
	4.1	Effect of Initial Conditions	28
	4.2	Transient Resonance	34
	4.3	Catastrophic Yaw	40
	4.4	Roll Break-Out	47
V	CONCLUSIONS		
	5.1	Summary and Significance of Results	48
	5.2	Recommendations for Further Work	50
	LIST OF REFERENCES		51
	APPENDIX A		53

LIST OF FIGURES

Figure		Page
2.1	Aeroballistic Axis System	7
2.2	Tricyclic Motion	12
2.3	Trim Amplification	14
3.1	Projectile with an Offset Center-of-Mass	18
3.2	Locus of Equilibrium Solutions for $\dot{\phi}_S$=3.0,h=0.1	22
4.1	Normal Lock-In	31
4.2	Reverse Lock-In	32
4.3	Phase-Plane Representation of Lock-In Solution	34
4.4	Normal Transient Resonance	38
4.5	Reverse Transient Resonance	39
4.6(a)	Root Locus of Lock-In Solution with Parameter $\hat{K}_P$	44
4.6(b)	Root Locus of Lock-In Solution with Parameter $\hat{H}$	44
4.7	Catastrophic Yaw	46

LIST OF TABLES

Table		Page
3.1	Stability Matrix	24
3.2	Stability of Equilibrium Solutions	26
4.1	Stable Lock-In Solutions	36
4.2	Effect of Parameter Variation on Equilibrium Solutions	42

LIST OF SYMBOLS

C_D =drag force coefficient

$C_{L\alpha}$ $=C_{N\alpha} - C_D$

C_{ℓ_p} =roll damping moment coefficient

C_{M_o} =asymmetry moment coefficient

$C_{M_{p\alpha}}$ =Magnus moment coefficient

C_{N_o} =asymmetry force coefficient

$C_{N\alpha}$ =normal force coefficient

F_N =normal force due to radially offset center-of-mass

F_X, F_Y, F_Z $=\tilde{X}\tilde{Y}\tilde{Z}$ components of aerodynamic force

G $=\hat{K}_\theta \delta_{TR}$

H $=(\rho Sl/2m)[C_{L\alpha} - C_D - k_t^{-2}(C_{M_q} + C_{M_{\dot{\alpha}}})]$

h $=(\hat{H} - \sigma\hat{T})/(1-\sigma)$

I =transverse moment of inertia

I_X =axial moment of inertia

K_1, K_2 =amplitudes of nutation and precession modes, respectively

K_3 =trim angle amplitude

K_p $=-(\rho Sl^3/2I_X)[C_{\ell_p} + k_a^2 C_D]$

K_θ $=(\hat{r}_c C_{N\alpha}/2)/[C_{\ell_p} + k_a^2 C_D]$

k_a^2 $=I_X/ml^2$

k_t^2 $=I/ml^2$

L, M, N $=\tilde{X}\tilde{Y}\tilde{Z}$ components of aerodynamic moment

L =roll moment due to radially offset center-of-mass

l =reference length (diameter)

M $=(\rho Sl^3/2I)C_{M_\alpha}$

M_A $=-(\rho Sl^3/2I)C_{M_o}$

M_T =trim moment

m =mass

p, q, r =$X\tilde{Y}\tilde{Z}$ components of missile angular velocity

$\hat{r}_c$ =radial offset of the center-of-mass, calibers

S =reference area

s = $\int_0^t (V/l)\, dt$

s_g =gyroscopic stability factor

T =$(\rho S l/2m)[C_{L_\alpha} + k_\alpha^{-2} C_{M_{p\dot{\alpha}}}]$

t =time

u, v, w =$X\tilde{Y}\tilde{Z}$ components of V

V =missile velocity

XYZ =missile-fixed axes

$X\tilde{Y}\tilde{Z}$ =aeroballistic axes

$\tilde{\alpha}, \tilde{\beta}$ =angles of attack and sideslip in the aeroballistic system, respectively

δ =absolute value of ξ and $\tilde{\xi}$

δ_f =differential fin cant angle

δ_{TR} =$\delta_{TO}/|h|$

δ_{TO} =M_A/M

ζ =ξ/δ_{TR}

θ =orientation angle of ξ

$\tilde{\theta}$ =orientation angle of $\tilde{\xi}$

θ^* =orientation angle of $\dot{\xi}_0$

λ_1, λ_2 =damping of nutation and precession modes, respectively

ω_1, ω_2 =nutation and precession frequencies, respectively

ξ =complex angle of attack in the missile-fixed system,
$= \beta + i\alpha = \delta e^{i\theta}$

$\tilde{\xi}$ =complex angle of attack in the aeroballistic system,
$= \tilde{\beta} + i\tilde{\alpha} = \delta e^{i\tilde{\theta}}$

ξ_T =constant trim angle value of ξ

ρ =air density

σ =I_x/I

τ =$[-M/(1-\sigma)]^{\frac{1}{2}} s$

Φ =roll angle

Φ_M =asymmetry moment orientation angle

Φ_N =asymmetry force orientation angle

Superscripts

$(-)$ =complex conjugate

$(\hat{})$ =$[-(1-\sigma)M]^{1/2}$ $(')$

$(')$ =$d(\ )/d\tau$

=$d(\ )/dt$ (in Chapter 2)

$(\ )'$ =$d(\ )/ds$

Subscripts

e =equilibrium value

R =resonance

s =steady-state value

Chapter I

INTRODUCTION

Finned projectiles have today gained common use as military ordnance, especially as anti-tank ammunition. Such projectiles (high Kinetic Energy weapons) are fired at very high velocities (over 1500 m/s) and are intended to pierce tank armour by their sheer speed, and consequent energy. Given the need for high muzzle velocities, these projectiles are preferred to be fin-stabilized in contrast to spin-stabilized artillery shells and projectiles. The use of fin-stabilization has, however, brought into focus a number of problems which, although identified long ago, were not considered of sufficient practical significance. Among these are roll resonance and the associated problem of roll lock-in.

Finned projectiles are designed to be inherently statically stable and, hence, do not need to be spun. Such an unspun projectile which is symmetric exhibits precessional and nutational motion. Most projectiles of this type are dynamically stable, that is, the precessional and nutational modes damp out with time. However, slight configurational asymmetries always exist. "Slight configurational asymmetry" refers to missiles where the assumption of rotational

symmetry is valid for aerodynamic derivatives and moments of inertia; however, significant asymmetric aerodynamic moments are generated so as to trim the unspun projectile at an angle of attack (sometimes called the "asymmetry angle").

Projectiles are usually designed with marginal static stability that results in small natural frequencies in pitch and yaw. Moreover, small asymmetries or disturbances can easily set an initially unspun projectile into a roll. Such an accidentally produced roll rate may readily match with the low natural pitch-yaw frequency. This results in magnification of the trim angle, and the projectile undergoes large-amplitude yawing motion. This is called roll resonance and may lead to instability.

A common solution to avoid roll resonance is to cant the fins and deliberately roll the projectile through the resonance region. Surprisingly, many flight failures were observed when the roll rate failed to build up to the equilibrium (design) value corresponding to the fin cant. Instead, the roll rate was seen to get locked in at resonance; this phenomenon is termed roll lock-in. The observed lock-in tendencies could not be explained based on the existing linear aeroballistic theory. The theory predicted that the roll rate would vary through the resonance region and the projectile would attain only a fraction of the maximum (resonant) amplitude. The actual disturbances were much larger. To satisfactorily explain the

occurrence of roll lock-in and to account for the discrepancies between the linear theory and actual flight experiences, various nonlinear formulations have been suggested in the literature. The present study is also a step in this direction.

Before proceeding with a summary of the scope and extent of the present study, a brief survey of existing literature is presented. A fairly complete linear theory of the pitching and yawing motion of spinning shells was first published by Fowler et al[1] in 1920. This was later refined by McShane et al[2] in 1953. The linear theory has been used in this form to date and a good description is available in textbooks[3,4]. A recent survey paper by Murphy[5] serves as an excellent guide to the field of "flight dynamics of missiles." It concentrates on various sources of dynamic instability and is of direct relevance to the present study. A survey paper by Platus[6] on ballistic re-entry vehicle dynamics also covers many related topics.

The concept of a "slightly asymmetric missile" was introduced by Nicolaides[7] in 1953. He modified the linear theory and applied it to analyze angular motion of such missiles and showed the possibility of occurrence of roll resonance. Murphy[8] predicted the influence of nonlinear forces and moments on a symmetric missile. The phenomena of "roll lock-in" and "catastrophic yaw" were put forward by Nicolaides[9] soon after. The mechanism of generation of

nonlinear moments causing these phenomena was explored by Price[10], Chadwick[11], and Barbera[12]. However, most of the effort was directed towards re-entry vehicles.

A more general analysis of the motion of asymmetric rolling bodies in the presence of nonlinear aerodynamics was presented by Murphy[13]. Using the method of slowly-varying parameters, Clare[14] was able to extend his solution to include resonance. However, both Murphy[13] and Clare[14] had assumed a constant spin rate. This constraint was later relaxed by Murphy[15], but the rolling moment was assumed to be linear. Thus, none of these efforts could explain roll lock-in.

Nayfeh and Saric[16] employed the method of multiple scales and solved the coupled nonlinear roll, pitch, and yaw equations to analyze roll resonance of a re-entry vehicle and to obtain necessary conditions for lock-in. Modeling and analysis of roll resonance and lock-in of re-entry vehicles was also taken up by Kevorkian[17], and Kevorkian and Lewin[18]. However, a recent work by Murphy[19] has gone a long way in presenting a lucid exposition of the theory of roll lock-in of finned projectiles.

The present study seeks to expand on the work of Murphy[19]. The question of stability of the equilibrium solution at lock-in obtained from the nonlinear system equations is considered in greater detail. Lock-in solutions for the case

of an offset centre-of-mass are investigated for varying sets of parameters. The importance of both stable and unstable lock-in solutions is brought out. Other anomalous roll behavior of rolling finned projectiles like transient resonance is also considered. Finally, we take a look at the phenomenon of catastrophic yaw and at the possibility of break-out from lock-in of finned projectiles.

The remainder of this thesis is arranged as follows. Chapter 2 sets down the equations of motion of a rolling projectile in an aeroballistic coordinate frame. This is followed by a brief description of the main results of the linear aeroballistic theory. Chapter 3 discusses the lock-in theory and investigates the stability of lock-in solutions. The results of the present study covering the phenomena of roll resonance and lock-in, transient resonance, catastrophic yaw, and roll break-out have been put together in Chapter 4. The thesis ends with a summary of its chief contributions, and with suggestions for future work based on these foundations.

Chapter II

LINEAR THEORY

2.1 Aeroballistic Axes

Aeroballistic axes (Fig.2.1) provide a convenient non-spinning coordinate system for the study of rolling missiles. The X-axis faces forward along the projectile principal axis while the $\widetilde{Y}$-axis lies perpendicular to the X-axis and is initially in the horizontal plane. The $\widetilde{Z}$-axis is at right angles to both the X and $\widetilde{Y}$ axes, and points initially in the downward direction so as to form a right-handed coordinate system. The axis system pitches and yaws with the projectile, but has a zero roll rate. Then, after the initial instant, the $\widetilde{Y}$-axis may be displaced from the horizontal plane by the pitching and yawing motion of the projectile[5]. The missile-fixed axis system (X,Y,Z) is also shown in Fig.2.1.

2.2 Equations of Motion

The equations of motion for a basically symmetric missile[19] in the aeroballistic system are as follows:

$$F_X = m (\dot{u} + wq - rv)$$
$$F_Y = m (\dot{v} + ru)$$
$$F_Z = m (\dot{w} - qu) \qquad \ldots(2.1)$$

YZ	: MISSILE-FIXED AXIS
$\tilde{Y}\tilde{Z}$	: AEROBALLISTIC AXIS

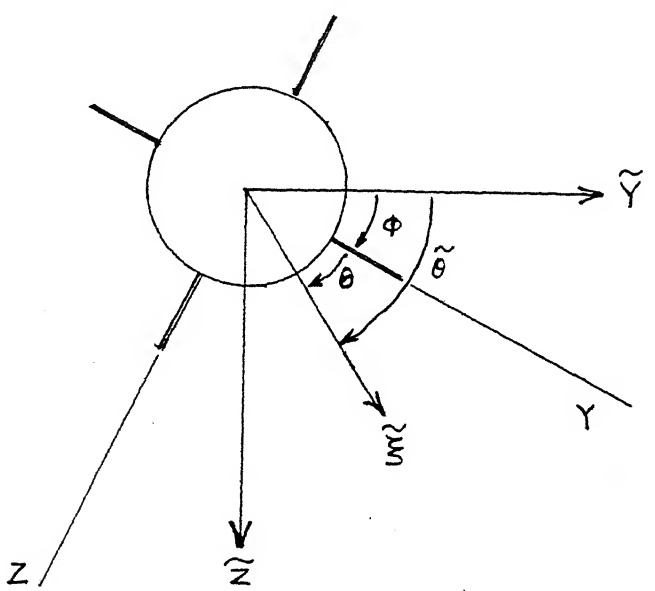

AFT LOOKING FORWARD

FIG. 2.1: AEROBALLISTIC AXIS SYSTEM

$$L = I_x \dot{p} \qquad \ldots(2.2)$$

$$M = I\,\dot{q} + I_x pr$$

$$N = I\,\dot{r} - I_x qp \qquad \ldots(2.3)$$

Linear aeroballistic theory seeks to solve the equations of angular motion of a projectile under the assumptions of

(i) constant roll rate,

(ii) small angle of attack and linear aerodynamics,

(iii)constant total projectile velocity.

In addition, the force equations (2.1) are taken to be identically satisfied.

For a symmetric missile,

$$q = \dot{\tilde{\alpha}} \ , \ r = -\dot{\tilde{\beta}} , \qquad \ldots(2.4)$$

where $\tilde{\alpha} = w/u$ and $\tilde{\beta} = v/u$.

The following expansions for the pitching and yawing moments are assumed [3,4]:

$$M = M_\alpha \tilde{\alpha} + M_{\dot{\alpha}} \dot{\tilde{\alpha}} + M_q q + M_{p\beta} p\tilde{\beta}$$

$$N = N_\beta \tilde{\beta} + N_{\dot{\beta}} \dot{\tilde{\beta}} + N_r r + N_{p\alpha} p\tilde{\alpha} \qquad \ldots(2.5)$$

In addition, a body-fixed asymmetry will cause a trim moment M_T which will rotate with the projectile roll rate. (2.3) will now appear as under:

$$I\dot{q} + rpI_x - M_\alpha \tilde{\alpha} - M_{\dot{\alpha}} \dot{\tilde{\alpha}} - M_q q - M_{p\beta} p\tilde{\beta} = M_T \cos(pt)$$

$$I\dot{r} - qpI_x - N_\beta \tilde{\beta} - N_{\dot{\beta}} \dot{\tilde{\beta}} - N_r r - N_{p\alpha} p\tilde{\alpha} = M_T \sin(pt) \qquad \ldots(2.6)$$

A complex angle of attack is defined as $\tilde{\xi} = \tilde{\beta} + i\tilde{\alpha}$.

Also, the following equalities hold due to rotational symmetry:

$$M_\alpha = -N_\beta \qquad M_q = N_r$$
$$M_{\dot{\alpha}} = -N_{\dot{\beta}} \qquad M_{p\beta} = N_{p\alpha} \qquad \ldots(2.7)$$

(2.6) can now be combined by multiplying the second equation by 'i' and adding it to the first to give a single equation in the complex variable $\tilde{\xi}$.

$$\ddot{\tilde{\xi}} + \left(-ip\frac{I_x}{I} - \frac{M_q + M_{\dot{\alpha}}}{I}\right)\dot{\tilde{\xi}} + \left(-ip\frac{M_{p\beta}}{I} - \frac{M_\alpha}{I}\right)\tilde{\xi}$$
$$= i\frac{M_T}{I}\exp(ipt) \qquad \ldots(2.8)$$

Since p has been assumed constant, (2.8) is a linear differential equation with time-invariant coefficients and can be solved for the complex angle of attack, $\tilde{\xi}$. The trim moment appears on the right hand side of (2.8) and acts as a source of excitation.

2.3 Tricyclic Motion

Rewriting (2.8) as

$$\ddot{\tilde{\xi}} + N_1\dot{\tilde{\xi}} + N_2\tilde{\xi} = N_3\exp(ipt) \qquad \ldots(2.9)$$

a solution can be found as[3]

$$\tilde{\xi} = K_1\exp(m_1 t) + K_2\exp(m_2 t) + K_3\exp(ipt) \quad ..(2.10)$$

where

$$m_{1,2} = -\frac{N_1}{2} \pm \sqrt{\left(\frac{N_1}{2}\right)^2 - N_2}$$

$$= \lambda_{1,2} \pm i\,\omega_{1,2} \qquad ..(2.11)$$

K_1 and K_2 are obtained from the initial conditions while K_3 is given by[3]

$$K_3 = \frac{N_3}{(ip - m_1)(ip - m_2)}$$

$$= \frac{N_3}{\left[i(p-\omega_1) - \lambda_1\right]\left[i(p-\omega_2) - \lambda_2\right]} \qquad ..(2.12)$$

(2.11) on substituting for N_1 and N_2 from (2.8) gives

$$\lambda_{1,2} = \left(\frac{M_q + M_{\dot{\alpha}}}{2I}\right)(1 \pm \Delta) + \frac{M_{p\beta}}{I_x}\Delta \qquad ..(2.13)$$

$$\omega_{1,2} = \frac{pI_x}{2I}\left(1 \pm \frac{1}{\Delta}\right) \qquad ..(2.14)$$

where $\Delta = \dfrac{1}{\sqrt{1 - \frac{1}{s_g}}}$ and $s_g = \dfrac{(pI_x/2I)^2}{(M_\alpha/I)}$ ..(2.15)

For a statically stable (finned) projectile;

$s_g < 0$, $0 < \Delta < 1$.

Therefore, ω_1 is in the same sense as p and is larger in magnitude than ω_2 which is in a sense opposite to p. ω_1 is called the nutation frequency and ω_2 the precession frequency. The angular motion described by (2.10) consists

of three modes and is represented by three rotating vectors (Fig.2.2):

$$\text{NUTATION vector} : \quad \bar{K}_1 = \bar{K}_{10} \exp[(\lambda_1 + i\omega_1)t]$$
$$\phi_1 = \omega_1 t + \arg(\bar{K}_{10})$$

$$\text{PRECESSION vector:} \quad \bar{K}_2 = \bar{K}_{20} \exp[(\lambda_2 + i\omega_2)t]$$
$$\phi_2 = \omega_2 t + \arg(\bar{K}_{20})$$

$$\text{TRIM vector} : \quad \bar{K}_3 = \bar{K}_{30} \exp(ipt)$$
$$\phi_3 = pt + \arg(\bar{K}_{30}) \qquad ..(2.16)$$

The locus of the projectile tip in Fig.2.2 is sometimes called a yaw rosette. Examples of yaw rosettes are available in Ref[4].

2.4 Resonance

Since $\bar{K}_2$ rotates in a direction counter to the projectile roll motion, resonance is possible only for $p = \omega_1$, as seen from (2.12). For $p = \omega_1$, (2.14) yields:

$$\omega_1 = p_R = \left(\frac{p_R I_x}{2I}\right) + \sqrt{\left(\frac{p_R I_x}{2I}\right)^2 - \frac{M_\alpha}{I}}$$

which gives the resonance roll rate as

$$p_R = \frac{(-M_\alpha / I)^{1/2}}{\left(1 - \frac{I_x}{I}\right)^{1/2}} \qquad ..(2.17)$$

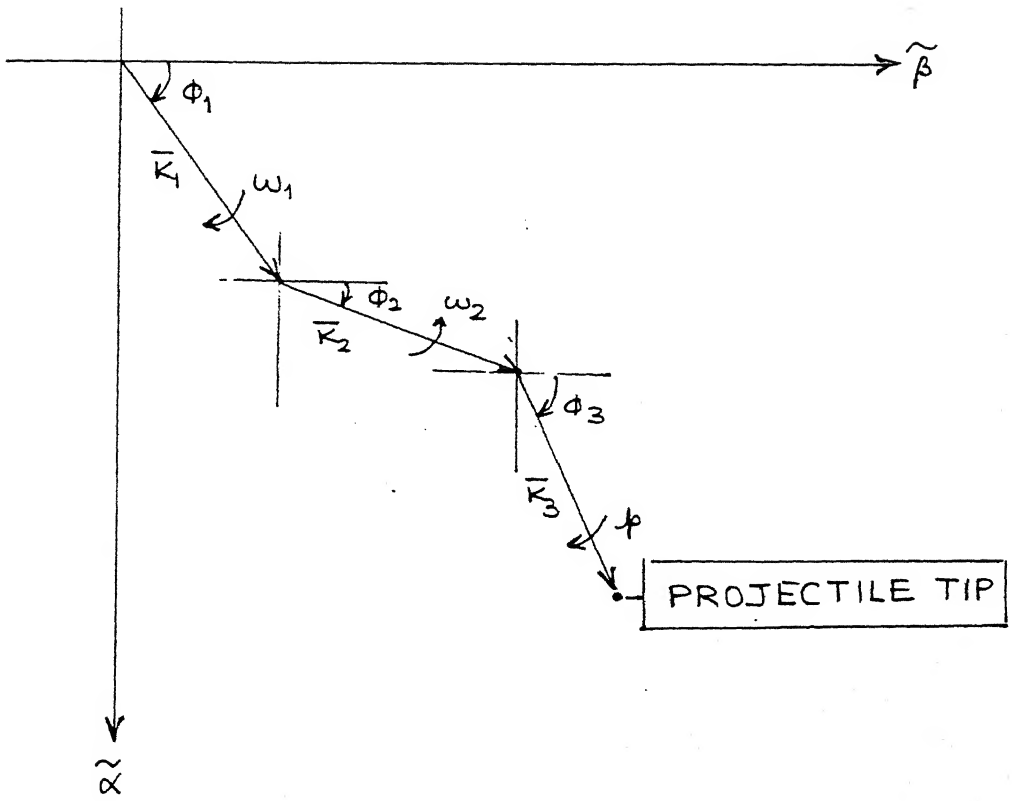

FIG.2.2: TRICYCLIC MOTION

Since $I_x/I \ll 1$ usually, the resonance roll rate can be seen to be very nearly equal to the projectile natural pitching frequency, $\sqrt{-M_\alpha/I}$. When the projectile roll rate is near the resonance frequency, the yaw rosette has an approximately circular pattern. Angular motion of this nature has been called lunar yawing motion[4].

Projectiles at resonance show bounded oscillations of large amplitude due to an increase in the magnitude of the trim angle of attack (K_3). Using (2.12), the amplification of the non-rolling trim can be expressed as[14]

$$\frac{K_3}{K_3\big|_{p=0}} = \frac{-M\alpha/I}{h_1 + ih_2} \qquad ..(2.18)$$

where $h_1 = \omega_2(p-\omega_1) + p(\omega_1 - p)$

$$h_2 = \lambda_2(\omega_1 - p) + \lambda_1(\omega_2 - p) \qquad ..(2.19)$$

The magnitude of the trim amplification is obtained from (2.18).

$$\left|\frac{K_3}{K_3\big|_{p=0}}\right| = \left[\frac{(-M\alpha/I)^2}{h_1^2 + h_2^2}\right]^{1/2} \qquad ..(2.20)$$

This can be seen from (2.19) and (2.20) to grow to a maximum at resonance ($p = \omega_1$). Fig.2.3 taken from Ref[5] shows the trim amplification at resonance. Thus, the linear theory is adequate to explain the occurrence of roll resonance.

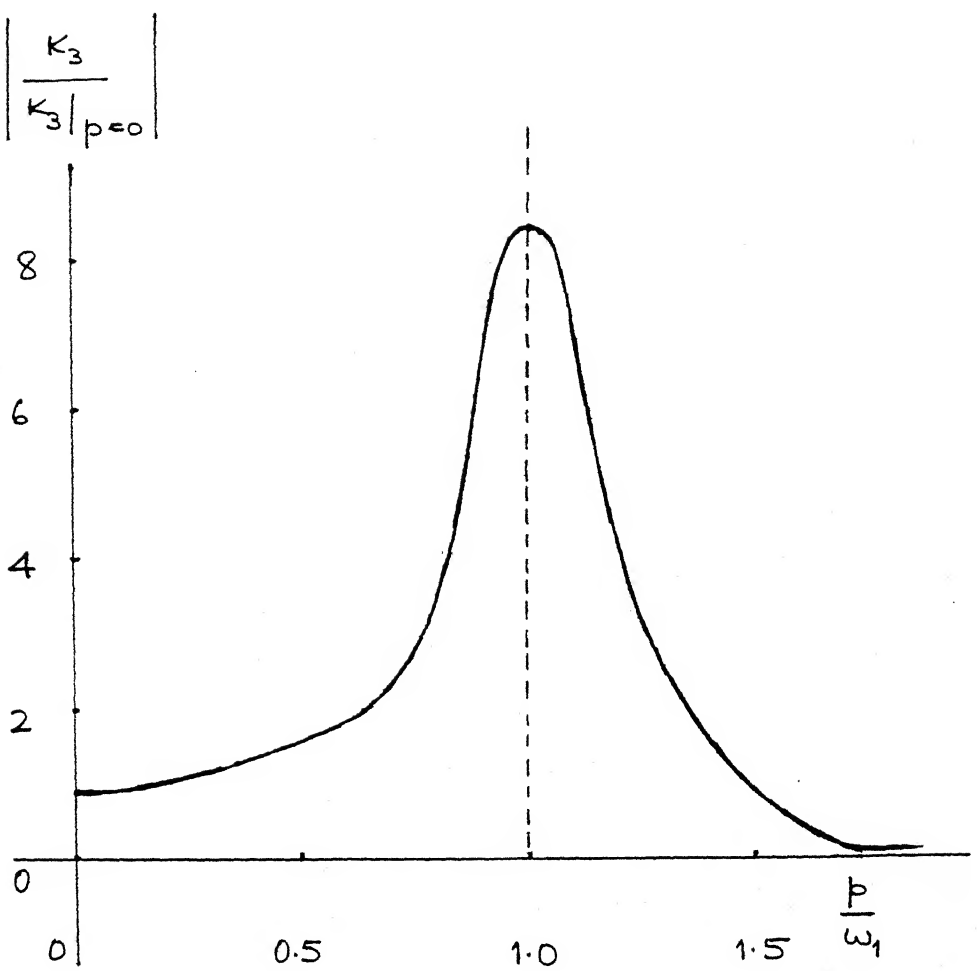

FIG. 2.3: TRIM AMPLIFICATION

In predicting the behavior of a projectile rolling through the resonance region, the variation of the roll rate cannot be overlooked. The linear theory, on the other hand, assumes a constant roll rate without which (2.8) will not be amenable to an analytic solution in a closed form. However, it seems plausible to apply the linear theory to the problem of passage through resonance of a rolling projectile by assuming the roll rate to be varying slowly. Then, one can use the roll rate at every instant as a constant in the linear pitch-yaw equation(2.8), and thereby obtain the resulting angle of attack at each instant given by (2.10). This approach, however, neglects any lag in the response due to the presence of damping forces. Notwithstanding this drawback, the above approach appears adequate to predict the behavior of a projectile in flight as it passes through resonance.

But as flight experiences showed[10,11], predictions based on the linear theory with the above modification were proven to be unsatisfactory. The theory was, in many cases, unable to explain observed flight behavior like roll lock-in and catastrophic yaw. This gives rise to the need to develop a more comprehensive theory. To that purpose, the assumption of constant roll rate is relaxed and some nonlinear terms are introduced in the linear equations of motion. This proves effective to explain the occurrence of roll lock-in as discussed in the following chapter.

Chapter III

LOCK-IN THEORY

3.1 Roll Equation

The main shortcoming of the linear theory has been seen to be its assumption of a constant roll rate. This must, therefore, be relaxed as the first step in the development of a lock-in theory. That requires the rolling moment in (2.2) to be non-zero. The rolling moment in its simplest form can be put down as comprising of two components: a roll-damping term, and a term due to fin cant.

$$L = L_p p + L_\delta \delta_f \qquad \ldots(3.1)$$

The pitch-yaw equation(2.8) retains its original form while the roll equation (2.2) with the rolling moment given by (3.1) is independent of $\tilde{\xi}$. Thus, it can be solved to give a steady-state roll rate

$$p_{ss} = - (L_\delta / L_p) \delta_f \qquad \ldots(3.2)$$

Now, (2.8) can be solved as before with $p = p_{ss}$. Thus, only one equilibrium solution is possible. This is called the design solution. The value of p_{ss} (and the resultant $\tilde{\xi}$) can be selected by the designer by using an appropriate degree of fin cant, δ_f.

It may be observed that the expansion assumed in (3.1) for the rolling moment is insufficient to predict the occurrence of lock-in. An induced roll moment, which is a function of the total angle of attack and the roll angle between a particular fin and the plane of the total angle of attack, has been suggested[9] to explain the phenomenon of roll lock-in. With this added term, (3.1) modifies to

$$L = L_p p + L_\delta \delta_f + L_\theta(\theta,\delta) \qquad ...(3.3)$$

where L_θ is the induced roll moment term. Now, (2.2) and (2.3) constitute a set of nonlinear equations and, in general, can have more than one steady-state equilibrium solution.

3.2 Center-of-Mass Offset

One source of an induced roll moment is a radially offset center-of-mass. Fig.3.1 shows the center-of-mass offset by a quantity $(l\hat{r}_c)$ in the Φ=0 plane (along the body-fixed Y-axis). The resultant rolling moment is given by

$$L_\theta = F_N.(l\hat{r}_c).\sin\theta \qquad ...(3.4)$$

The differential equations for the angular motion of a projectile can now be derived. A brief outline of their derivation is provided in Appendix A. We follow the notation of Ref[19].

The roll equation obtained from (2.2) and (3.3) is

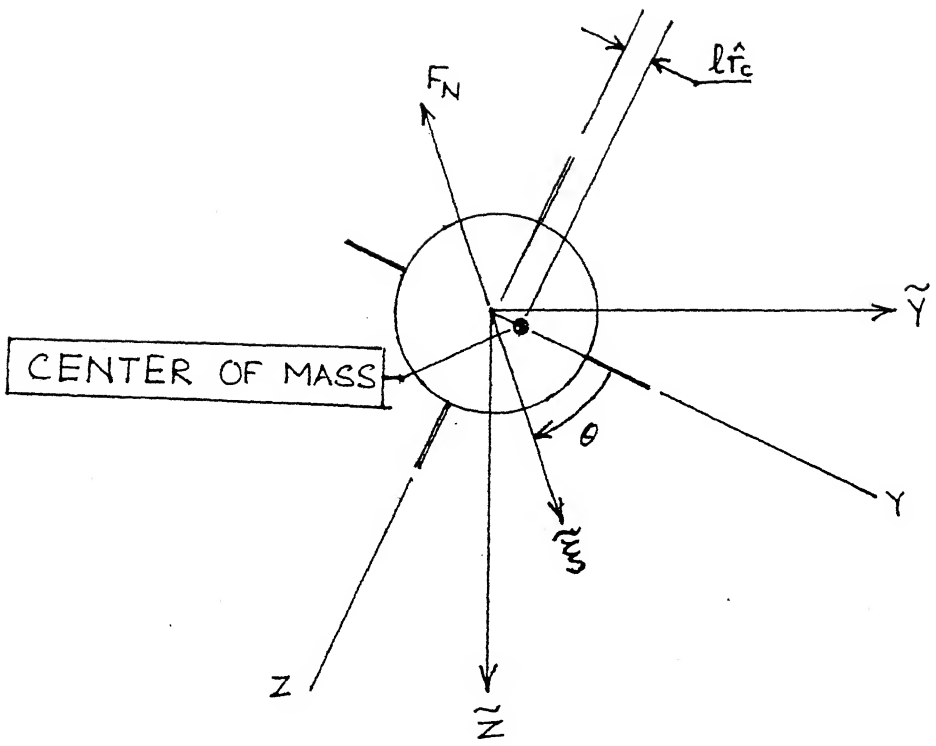

FIG.3.1: PROJECTILE WITH AN OFFSET CENTER-OF-MASS

$$\ddot{\phi} + \hat{K}_p[\dot{\phi} - \dot{\Phi}_s - iG\,(\zeta - \overline{\zeta})] = 0 \qquad \ldots(3.5)$$

The complete equation for the pitching and yawing motion derived from (2.1) and (2.3) is

$$\ddot{\zeta} + [\hat{H}+i(2-\sigma)\dot{\phi}]\dot{\zeta} + (1-\sigma)[1-\dot{\phi}^2+i\dot{\phi}h+i\ddot{\phi}] = (1-\sigma)|h|\exp(i\phi_M) \qquad \ldots(3.6)$$

The independent variable in equations (3.5) and (3.6) is a dimensionless time, τ, defined in equation (A.12) of Appendix A. By virtue of this definition, the roll rate in the above equations is scaled by the value of the resonance frequency. Thus, resonance is signified by a value of $|\dot{\phi}|=1$. Similarly, the complex angle of attack, ζ, is obtained by scaling ξ by the value of its magnitude at resonance as shown in equation (A.17) of Appendix A. The final term within the brackets in (3.5) stands for the induced roll moment. The excitation due to the trim in the pitch-yaw equation appears on the right hand side of (3.6). The dot (.) is used here, and henceforward, to denote derivative with respect to τ.

3.3 Equilibrium Solutions

The equilibrium solutions of (3.5) and (3.6) can be obtained by solving the following equations:

$$\dot{\phi}_e - \dot{\Phi}_s = iG\,(\zeta_e - \overline{\zeta}_e) \qquad \ldots(3.7)$$

$$\zeta_e = \frac{|h| \exp(i\Phi_M)}{1 - \dot{\phi}_e^2 + i\dot{\phi}_e h} \qquad \ldots(3.8)$$

(3.7) and (3.8) are obtained by setting $\dot{\zeta}$, $\ddot{\zeta}$, and $\ddot{\phi}$ in (3.5) and (3.6) to zero. In the above equations, 'h' represents the aerodynamic asymmetry with orientation Φ_M and 'G' stands for the magnitude of the center-of-mass offset.

(3.7) and (3.8) draw attention to some very significant points.

(i). If no configurational asymmetries exist, then the projectile will have a zero trim angle. This implies that h is zero. Therefore, there will be no amplification of trim at resonance and the complex angle of attack will have zero magnitude at equilibrium as seen from (3.8). It follows from (3.7) that the equilibrium roll rate is equal to the design value which implies that the problem of roll lock-in is ruled out.

(ii). No center-of-mass offset means G is zero, which from (3.7) implies that $\dot{\phi}_e$ is always equal to $\dot{\phi}_s$ (the design roll rate). For a non-zero trim ($h \neq 0$), resonance ($|\dot{\phi}|=1$) may occur with resultant trim amplification given by (2.20). But, the rolling moment in this case takes the form (3.1) and a lock-in solution requiring $\dot{\phi}_e \cong \pm 1$ is impossible. Physically, this implies that no steady-state equilibrium solution exists in the vicinity of resonance.

(iii).Even when h and G are both non-zero, (3.7) and (3.8) need not have a lock-in solution for all combinations of values of the parameters h, ϕ_M, and G.

The above statements are illustrated by an example. We choose

$$\dot{\phi}_S = 3.0,\ h = 0.1.$$

Four values of ϕ_M are considered.

$$\phi_M = 0^\circ,\ 90^\circ,\ 180^\circ,\ 270^\circ.$$

G is varied from 0 to 5.0 in steps of 0.1. To solve (3.7) and (3.8) for $\dot{\phi}_e$, the substitution of (3.8) in (3.7) leads to a fifth-order algebraic equation in $\dot{\phi}_e$. The real roots representing the equilibrium roll rates ($\dot{\phi}_e$) obtained by solving this equation for the range of values of G are shown in Fig.3.2.

The following inferences can be drawn from the figure:

A design solution, S, exists near the design value ($\dot{\phi}_S$=3.0) in each of the four cases for all values of G.

Lock-in solutions ($\dot{\phi}_e \cong \pm 1$) exist only for values of G greater than a particular minimum value. This minimum value is different in each case.

Lock-in solutions are of two types: normal resonance, N, ($\dot{\phi}_e \cong .+1$) and reverse resonance, R, ($\dot{\phi}_e \cong .-1$).

Both the N and R types of lock-in solutions always appear in pairs.

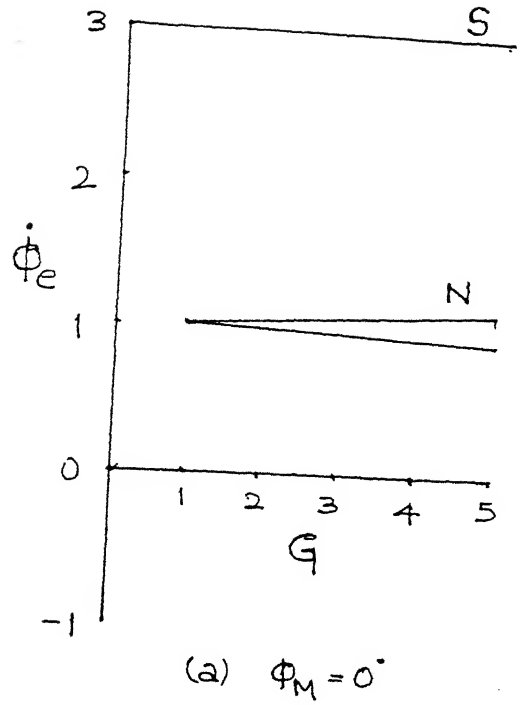

(a) $\Phi_M = 0°$

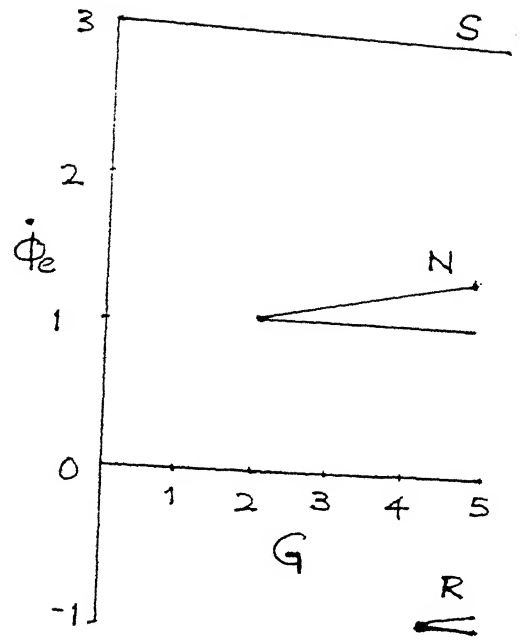

(b) $\Phi_M = 90°$

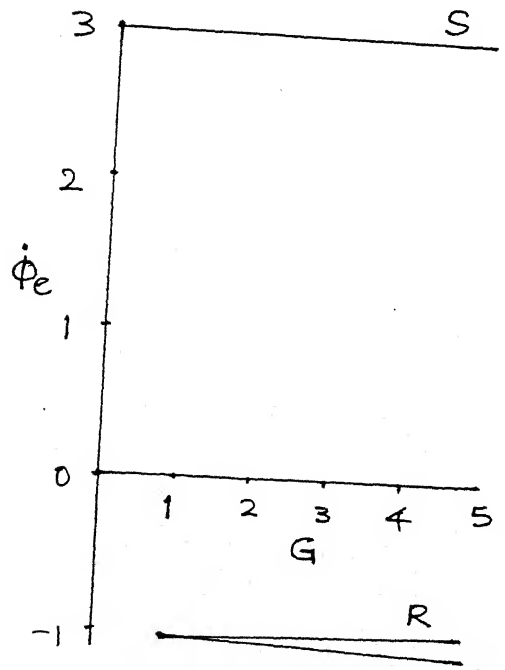

(c) $\Phi_M = 180°$

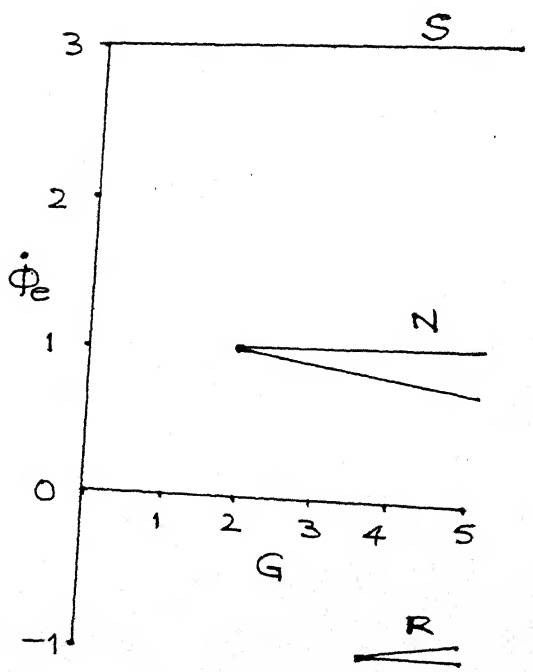

(d) $\Phi_M = 270°$

FIG. 3.2: LOCUS OF EQUILIBRIUM SOLUTIONS FOR $\dot{\Phi}_S = 3.0$, $h = 0.1$.

If an equilibrium solution exists at resonance, it may or may not be stable. The question of stability of equilibrium solutions is addressed next.

3.4 Lock-in Stability

We make use of Lyapunov's first method to investigate the stability of the equilibrium solutions of (3.5) and (3.6). Following Ref[19], we assume a small perturbation of an equilibrium state.

$$\dot{\Phi} = \dot{\Phi}_e + \eta_1$$
$$\zeta = \zeta_e + \eta_2 + i\eta_3$$
$$\dot{\eta}_2 = \eta_4$$
$$\dot{\eta}_3 = \eta_5 \qquad \ldots(3.9)$$

(3.5) and (3.6) can be cast as a system of five first-order differential equations. In vector notation,

$$\dot{\underline{x}} = \underline{f}(\underline{x}) \qquad ..(3.10)$$

Using (3.9), (3.10) can be written as

$$\dot{\underline{\eta}} = A\,\underline{\eta} + \underline{g}(\underline{\eta}) \qquad ..(3.11)$$

where $\underline{g}(\underline{\eta})$ represents higher-order terms. The elements of the 5x5 matrix A, called the stability matrix, are listed in Table 3.1[19]. Incidentally, some of the terms appearing in the stability matrix of Ref[19] are erroneous and they have been corrected in Table 3.1.

TABLE 3.1 STABILITY MATRIX

$$
\begin{bmatrix}
-\hat{K}_p & 0 & -2G\hat{K}_p & 0 & 0 \\
0 & 0 & 0 & 1 & 0 \\
0 & 0 & 0 & 0 & 1 \\
\left[2\dot{\phi}_e \mathrm{Re}(\zeta_e) + \mathrm{Im}(\zeta_e)(h-\hat{K}_p)\right] \cdot (1-\sigma) & -(1-\sigma)(1-\dot{\phi}_e^2) & (1-\sigma)\left[h\dot{\phi}_e - 2\hat{K}_p G\,\mathrm{Im}(\zeta_e)\right] & -\hat{H} & (2-\sigma)\dot{\phi}_e \\
\left[2\dot{\phi}_e \mathrm{Im}(\zeta_e) - \mathrm{Re}(\zeta_e)(h-\hat{K}_p)\right] \cdot (1-\sigma) & -(1-\sigma)\cdot h\dot{\phi}_e & (1-\sigma)\left[-(1-\dot{\phi}_e^2) + 2\hat{K}_p G\,\mathrm{Re}(\zeta_e)\right] & -(2-\sigma)\dot{\phi}_e & -\hat{H}
\end{bmatrix}
$$

(3.11) can be approximated by its linear part to study its stability characteristics provided $\underline{g(\eta)}$ is negligible, which is usually the case. In the linear approximation,

$$\dot{\underline{\eta}} = A\,\underline{\eta} \qquad ..(3.12)$$

The condition for stability requires that all the eigenvalues of matrix A have negative real parts.

For an investigation of equilibrium solutions and their stability, one value of G is selected for each of the four cases depicted in Fig.3.2. In addition to the earlier parameters, the following parameters are selected to have the values given below:

$$\hat{K}_p = 0.1,\ \hat{H} = 0.1,\ \sigma = 0.1.$$

Equilibrium solutions are obtained by solving (3.7) and (3.8) for the roll rate and complex angle of attack respectively. These are listed in Table 3.2 for all the four cases considered. The stability matrix, A, for an equilibrium state is obtained by evaluating the elements in Table 3.1. The stability of the equilibrium solution is, then, determined by the eigenvalues of the resulting matrix. The equilibrium solutions tabulated in Table 3.2 are classified as under:

SD	:	Stable - Design solution
SN	:	Stable - Normal Resonance solution
SR	:	Stable - Reverse Resonance solution
U	:	Unstable solution

TABLE 3.2 STABILITY OF EQUILIBRIUM SOLUTIONS

Φ_M	G	SOLUTIONS			CLASSIFICATION
		$\dot{\Phi}_e$	Re(ζ_e)	Im(ζ_e)	
0°	2.0	0.950	-0.5261	0.5126	SN
		1.050	0.4761	0.4877	U
		2.998	0.0125	0.0005	SD
90°	3.0	1.020	-0.8474	0.3357	SN
		1.129	-0.1280	0.3115	U
		2.920	-0.0005	0.0133	SD
180°	3.0	-1.034	-0.4469	0.6682	SR
		-0.963	0.4992	0.6619	U
		3.003	-0.0125	-0.0005	SD
270°	5.0	-0.976	-0.8289	0.4028	SR
		-0.862	-0.1545	0.3889	U
		0.754	0.0393	0.2249	U
		0.990	0.9709	0.1952	U
		3.115	0.0004	-0.0115	SD

PARAMETERS: $\dot{\phi}_s = 3.0$, $h = 0.1$, $\hat{H} = 0.1$, $\hat{K}_p = 0.1$, $\sigma = 0.1$.

The following observations can be made from Table 3.2:

For every stable lock-in solution, there exists an unstable solution whose equilibrium roll rate is very near that of the stable lock-in solution.

The design solution in each case is stable. Thus, all the cases under consideration show two stable solutions. For a different set of parameters, the number of stable solutions obtained may be different from two.

A nonlinear system may approach any one of its many possible stable states or diverge to infinity. Thus, for a nonlinear system with two stable solutions, it is impossible to predict a priori which of the two solutions will occur once the system is set in operation. In the context of the examples in Table 3.2, the projectile may attain the design solution or it may find itself at a stable resonance solution. This distinction is influenced solely by one factor, viz. the initial conditions at launch. This is taken up in the next chapter where the conditions under which a projectile does get locked in are considered.

Chapter IV

RESULTS AND DISCUSSION

In nonlinear systems, which one of the many possible equilibrium solutions actually occurs depends on the initial conditions. The final equilibrium state attained for a certain set of initial conditions can be determined only by studying the response of the system obtained by solving its equations of motion. For a given a set of initial conditions, the response of a projectile in flight can be obtained from a numerical integration of the system of equations (3.10). The numerical scheme used in the present study is a fourth-order Runge-Kutta-Gill method. Using the above procedure, we first investigate the occurrence of roll lock-in. Following this, the phenomena of transient resonance, catastrophic yaw, and roll break-out are studied for finned projectiles.

4.1 Effect of Initial Conditions

The initial conditions for a projectile are the roll rate, the complex angle of attack, and the complex angular velocity at launch. To study responses corresponding to all possible initial conditions is clearly impracticable. Instead, a realistic set of values was considered. The

initial roll rate ($\dot{\phi}_o$) and the initial complex angle (ζ_o) were taken to be zero[19], while the initial complex angular velocity ($\dot{\zeta}_o$) was varied.

$$\dot{\phi}_o = \zeta_o = 0$$
$$\dot{\zeta}_o = |\dot{\zeta}_o| \exp(i\theta^*) \qquad \ldots(4.1)$$

where θ^* is the orientation of the initial total angular velocity ($\dot{\zeta}_o$).

The following values were chosen for $|\dot{\zeta}_o|$:

$$|\dot{\zeta}_o| = 0.1,\ 0.2,\ 0.5,\ 1.0.$$

For each of the above values, θ^* was set at

$$\theta^* = 0^\circ,\ 90^\circ,\ 180^\circ,\ 270^\circ.$$

Thus, a total of sixteen different initial conditions were tested for each case listed in Table 3.2.

The results of the study are as given below. Cases (a), (b), (c), and (d) refer to the four cases in Table 3.2 corresponding to Fig.3.2.

In cases (a) and (c), the design solution occurs for each of the sixteen assumed set of initial conditions.

In case (b), the normal resonance solution was seen only for $|\dot{\zeta}_o|=1.0$, $\theta^*=0^\circ$. All other initial conditions led to the design solution. For comparision, two sets of initial conditions were chosen, one leading to resonance and the other yielding the design solution. The value of $|\dot{\zeta}_o|$ was kept fixed at 1.0. For $\theta^*=0^\circ$, we get the normal

lock-in solution and $\theta^*=180^\circ$ gives the design solution. The roll (spin) response and the yaw response corresponding to these initial conditions are shown in Fig.4.1. The figure highlights two significant results. First, the totally different nature of the response for two different sets of initial conditions (parameters held constant) is brought out very clearly. Second, the yaw response shows the large magnitude of the total angle of attack at equilibrium for the resonance solution. This is in contrast to the yaw response for the design solution which can be seen to damp out with time.

In case (d), $|\dot{\xi}_o|=1.0$, $\theta^*=270^\circ$, leads to the reverse resonance solution while the design equilibrium state is reached for the rest of the initial conditions. The roll and yaw responses in this case for $|\dot{\xi}_o|=1.0$ are shown in Fig.4.2. Different initial conditions for reverse lock-in ($\theta^*=270^\circ$) and for the design solution ($\theta^*=90^\circ$) in Fig.4.2 again indicate the vastly different nature of the response. As in case (b), similar inferences about the nature of the response can be drawn from Fig.4.2.

Based on observations such as mentioned for cases (b) and (d) above, designers have been cautioned[5] to avoid resonance. Catastrophic effects of large angle of attack amplification, range shortening from increased drag, and structural failure have been mentioned[6] as the disastrous

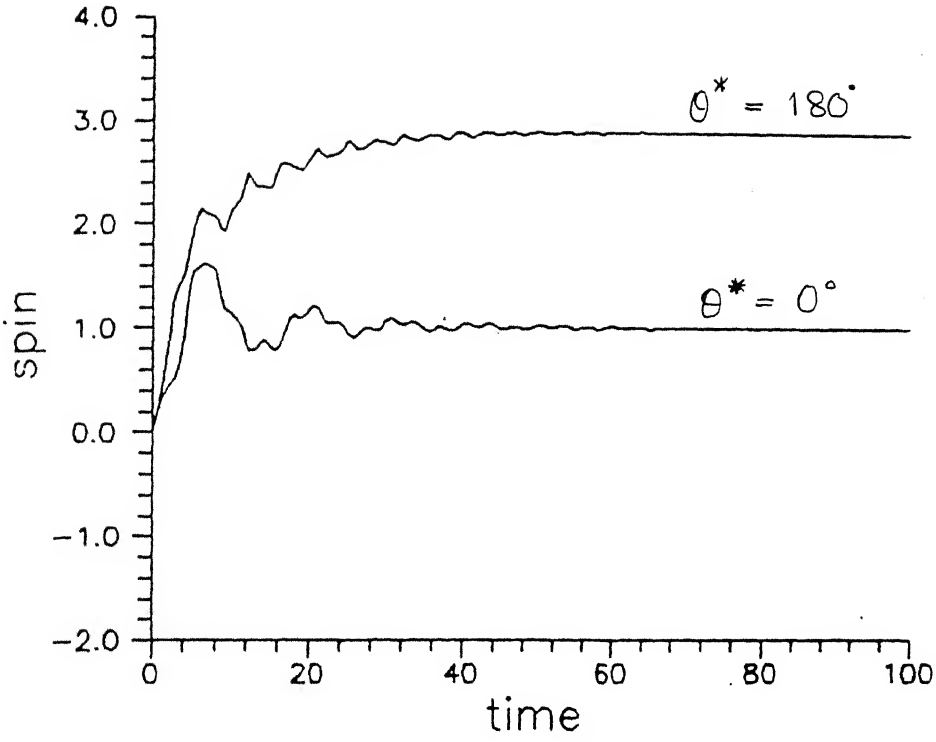

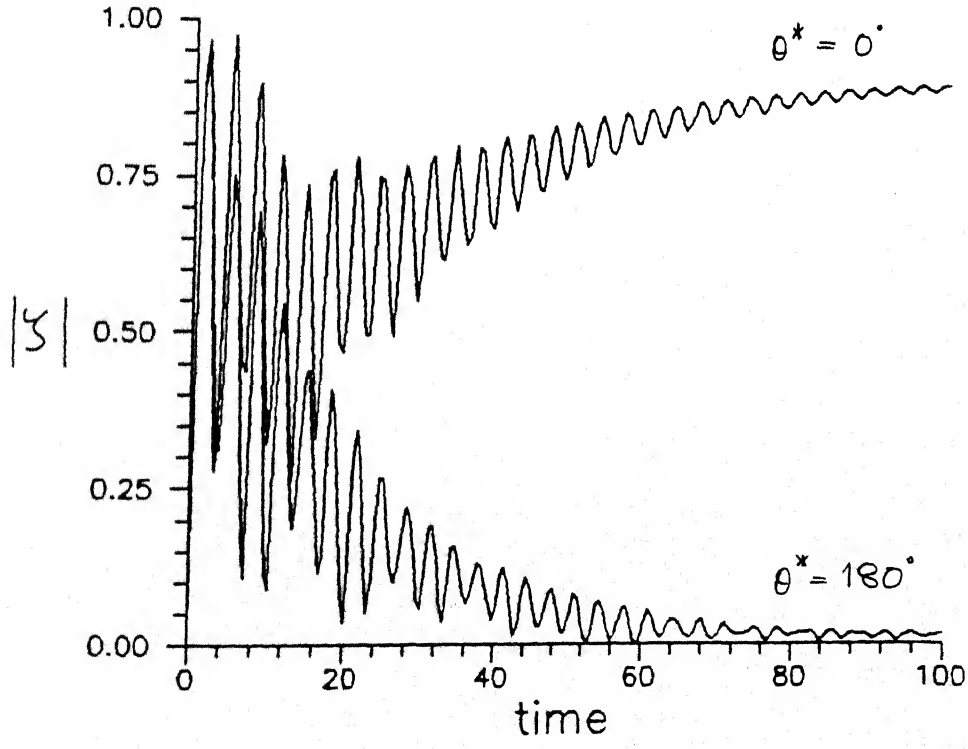

FIG. 4·1: NORMAL LOCK-IN

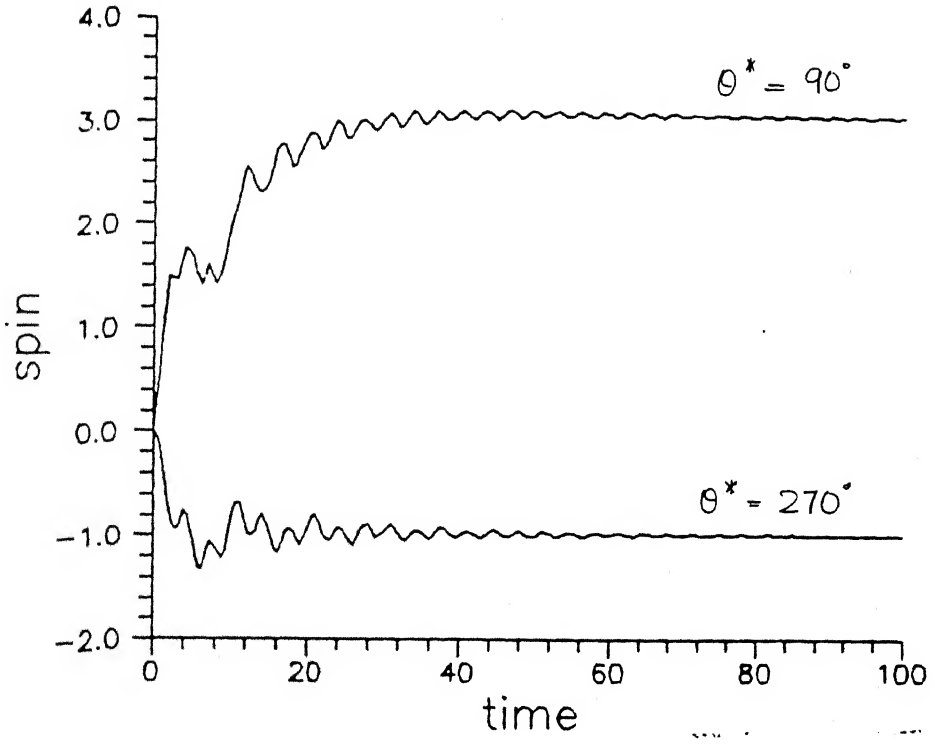

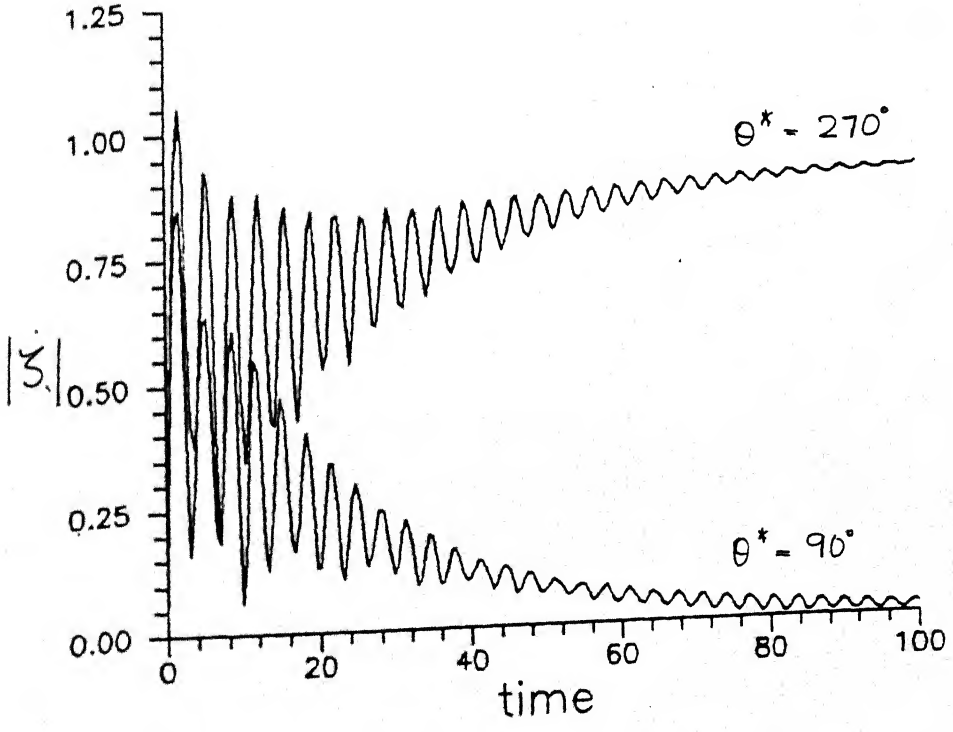

FIG. 4-2: REVERSE LOCK-IN

effects of roll lock-in. However, our study suggests that the occurrence of stable resonance solutions is not very common. For example, of the sixty-four sets of initial conditions considered in the present study, only two lead to a lock-in solution.

In order to explain why lock-in solutions occur so rarely, we recall that resonance solutions never occur in isolation and that an unstable solution always exists near every stable lock-in solution. While it is not possible to provide a topological portrait of the trajectories for a fifth-order system, many of the points can be made by using a two-dimensional phase-plane picture. As an example, consider Fig.4.3 which shows an unstable saddle point, P, near a stable focus, Q. The point Q can be taken to represent a stable resonance solution with an adjacent unstable solution shown by P. Along which trajectory a system will find itself depends on the initial conditions. Clearly, only those trajectories that lie between A and A' can reach the stable focus. The closer P and Q are to one another, the smaller will be the gap between A and A', and fewer trajectories will find their way to the stable focus, Q. This underlines the importance of the nature and location of all solutions, stable and unstable, in a nonlinear analysis.

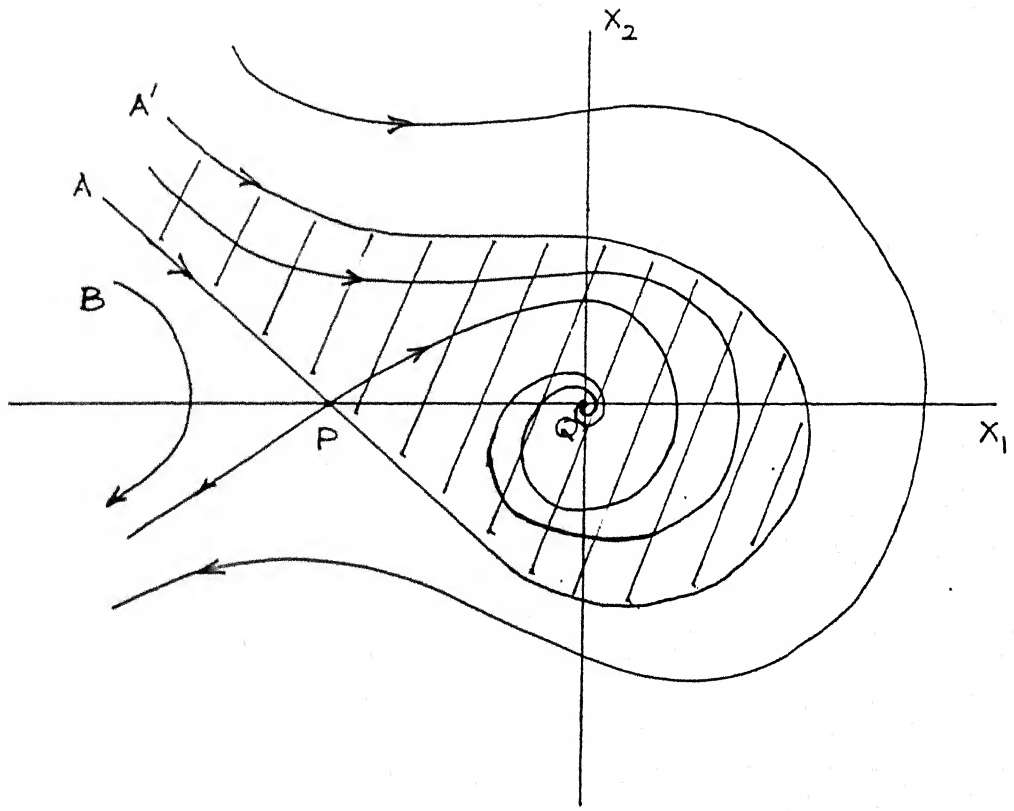

FIG.4.3: PHASE-PLANE REPRESENTATION OF LOCK-IN SOLUTION

4.2 Transient Resonance

As concluded from the previous discussion, a projectile may lock in at resonance for only a few initial conditions. However, its motion may still be significantly affected as it passes through the resonance region and the effect depends on the time spent at resonance condition. Depending on the orientation of the asymmetries, the nonlinear roll moment in (3.4) may either speed up or slow down the rolling motion of a projectile passing through resonance. As a result, the roll rate could linger at the resonance value for some time before building up to the design value. This phenomenon is termed transient resonance[12]. In terms of Fig.4.3, this is represented by trajectories like B which pass near the resonance solution, Q, but are not attracted to it. It is conjectured that the projectile would experience yawing motion of increased amplitude during the period it is at resonance.

To investigate transient resonance, the following values of the parameters are used:

$$\dot{\phi}_S = 3.0, \quad h = 0.1, \quad \phi_M = 90^{\circ}.$$

Case A: $G = 0$ Case B: $G = 3.0$

For case A, G is zero and only one solution is possible (the design solution). For case B, G is 3.0. The stable solutions for this case are shown in Table 4.1. The eigenvalues obtained from the stability matrix of Table 3.1 are listed

TABLE 4.1 STABLE LOCK-IN SOLUTIONS

Φ_M	G	SOLUTIONS			EIGENVALUES
		$\dot{\Phi}_e$	Re(ζ_e)	Im(ζ_e)	
90°	0	3.000	0.0000	0.0000	-0.042 ± i 1.89
					-0.057 ± i 3.80
					-0.100
	3.0	1.020	-0.8474	0.3357	-0.085 ± i 0.69
					-0.045 ± i 1.91
					-0.038
		2.920	-0.0005	0.0133	-0.046 ± i 1.81
					-0.056 ± i 3.73
					-0.093
270°	0	3.000	0.0000	0.0000	-0.042 ± i 1.89
					-0.057 ± i 3.80
					-0.100
	5.0	-0.976	-0.8289	0.4028	-0.080 ± i 0.89
					-0.050 ± i 1.86
					-0.037
		3.115	0.0004	-0.0115	-0.036 ± i 1.99
					-0.059 ± i 3.91
					-0.108

PARAMETERS: $\dot{\Phi}_S = 3.0$, $h = 0.1$, $\hat{H} = 0.1$, $\hat{K}_p = 0.1$, $\sigma = 0.1$.

along with the solutions in Table 4.1. The roll and yaw responses obtained for cases A and B are depicted in Fig.4.4. Identical initial conditions are used for both the cases and are mentioned in the figure.

The roll rate in case A builds up smoothly to the design value while the roll rate in case B shows the transient resonance phenomenon. Thus, the roll response is as expected. However, the predicted amplification in the yaw response is not seen to occur. On the contrary, the oscillations for case B in Fig.4.4 show distinctly increased damping during the time the roll rate is passing through the resonance region. This can be explained by a comparision of the damping ratios calculated from the complex eigenvalue pairs in Table 4.1 which showed the solution at resonance to be more damped in yaw than the design solution.

To ensure that the result indicated by Fig.4.4 was not a special case, we consider another set of parameters as follows:

$\dot{\phi}_S = 3.0, \quad h = 0.1, \quad \phi_M = 270^{\circ}.$

Case A: G = 0 Case B: G = 5.0

Again, case A with G equal to zero will have only one solution (design solution). The stable solutions in case B are listed in Table 4.1 along with their eigenvalues. Fig.4.5 shows the roll and yaw responses for both cases A and B. The roll rate for case A builds up to the design value while for case B it spends some time in the vicinity

$|\bar{\xi}_0| = 0.6, \quad \theta^* = 0^\circ$

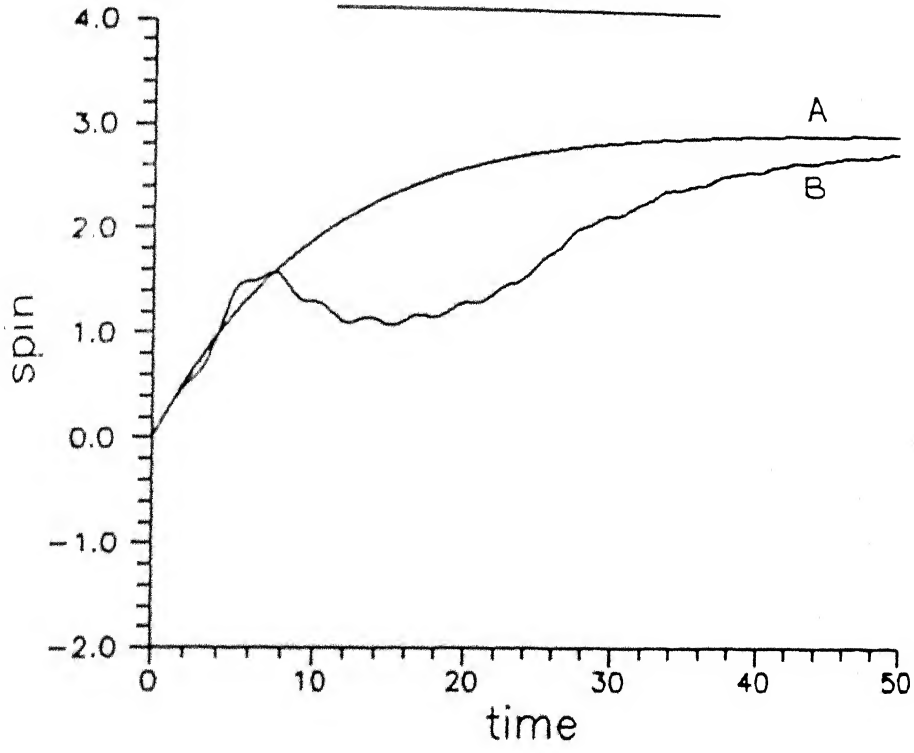

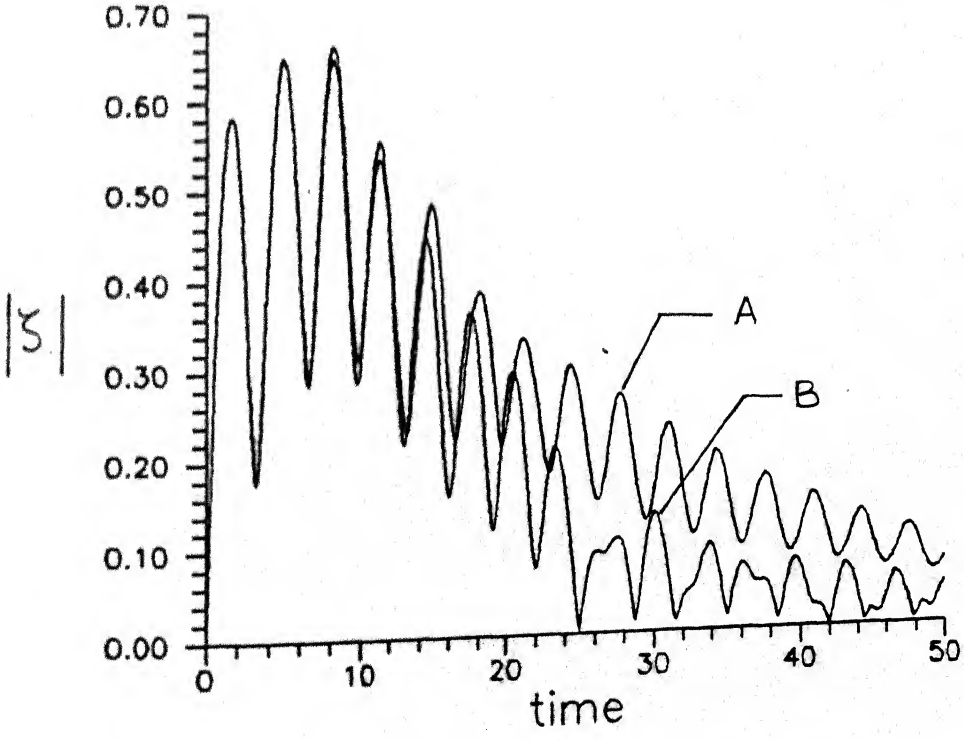

FIG.4.4: NORMAL TRANSIENT RESONANCE

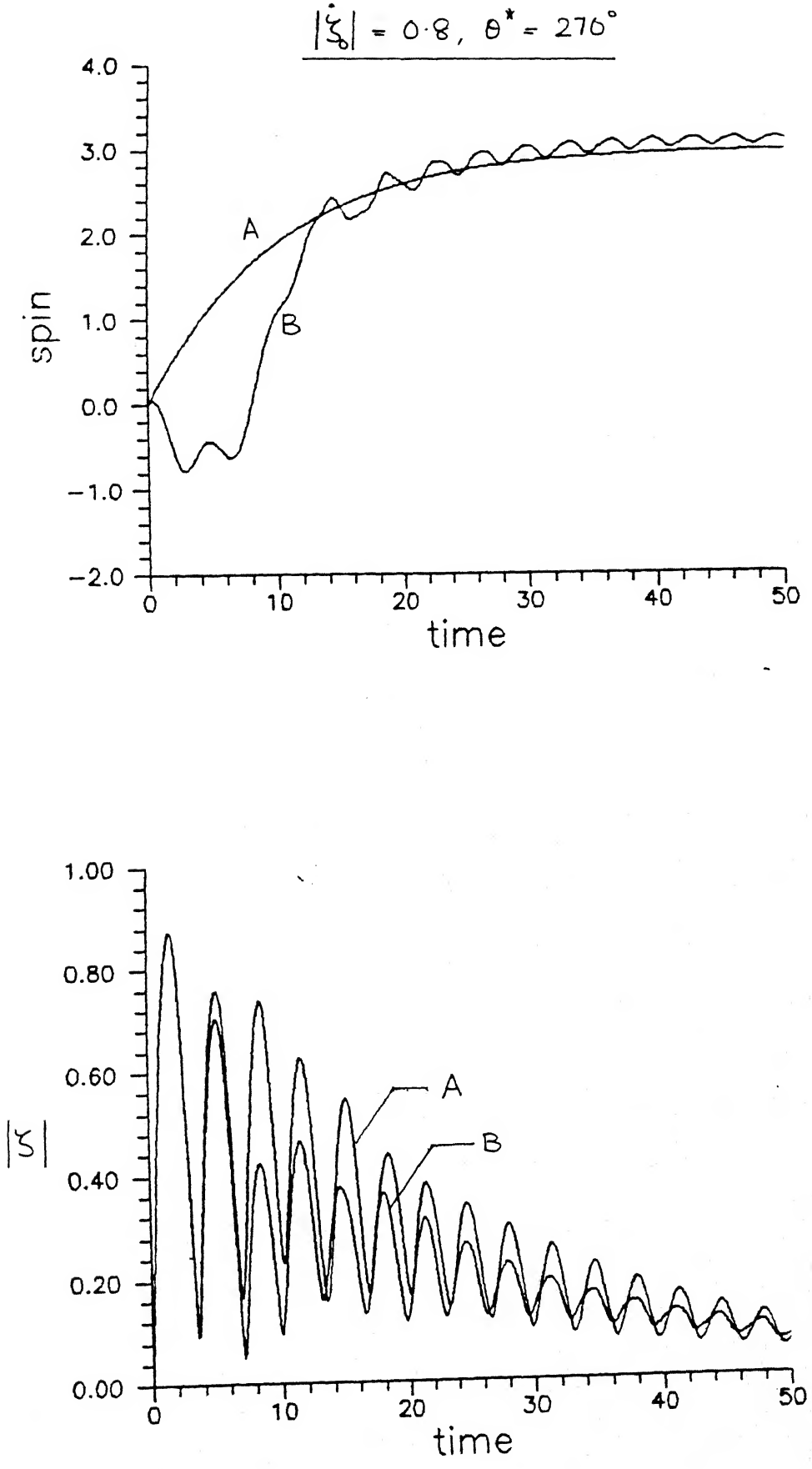

FIG.4.5: REVERSE TRANSIENT RESONANCE

of reverse resonance. As in Fig.4.4, one can observe an increase in the damping of the yaw response for case B in Fig.4.5. The eigenvalues in Table 4.1 for the solutions corresponding to the above set of parameters show the damping of the resonance solution to be more than that of the solution at the design value. Thus, it is likely that a response with increased damping would occur for other cases of transient resonance too.

This result is contrary to expectation and has not been reported in the literature so far. However, the actual response may be complicated by the presence of nonlinearities in the pitch-yaw equation (3.6) which have been neglected in the present analysis and can be verified only from wind-tunnel and flight tests. Induced side forces and moments arising in the flight of rolling missiles were predicted by Nicolaides[9] and have been described in the literature[20-22]. These are known to be highly nonlinear and could be significant enough to affect the flight of a projectile at resonance. Murphy[5] explained how these induced side moments could cause the "catastrophic yaw" postulated by Nicolaides[9].

4.3 Catastrophic Yaw

Finned projectiles experiencing high-amplitude lunar yawing motion are known to suffer from dynamic instability[4]. This results in an unlimited build-up of yaw called catastrophic

yaw. Many flight failures have been attributed[5] to this phenomenon.

Chadwick[11] describes the build-up to catastrophic yaw of a missile. The first step is attaining a stable rolling motion with the roll rate locked in at resonance. The roll rate then shows small oscillations about the equilibrium roll rate at lock-in. The lunar motion gives rise to induced side forces and moments, which destabilize the yawing motion of the projectile. If these induced moments can alter the stability in roll of the equilibrium solution at resonance, the projectile may break out of lock-in before the yaw build-up reaches a large value. This is the phenomenon of transient roll lock-in and break-out described by Barbera[12].

The present study explores the likelihood of occurrence of catastrophic yaw even in the absence of induced moments. To this end, we first investigate the effect of parameter variations on the stability of the equilibrium solution at resonance. The base values of the parameters assumed for the study are as follows:

$$\dot{\phi}_S = 3.0,\ h = 0.1,\ \phi_M = 90\ ,\ G = 5.0.$$

$$\hat{H} = 0.1,\ \hat{K}_p = 0.1,\ \sigma = 0.1.$$

The equilibrium solutions for this set of parameters are listed in Table 4.2. Only two of the five equilibrium states (corresponding to ϕ_e=1.011 and ϕ_e=2.861) are stable and the eigenvalues for these are also indicated in Table 4.2.

TABLE 4.2 EFFECT OF PARAMETER VARIATIONS ON EQUILIBRIUM SOLUTIONS

$\dot{\phi}_e$	Re(ζ_e)	Im(ζ_e)	EIGENVALUES	
			$\hat{H} = 0.1$, $\hat{K}_p = 0.1$	$\hat{H} = 0.08$, $\hat{K}_p = 0.2$
-1.086	0.2469	0.4079	UNSTABLE	UNSTABLE
-1.027	0.7583	0.4041	UNSTABLE	UNSTABLE
1.011	-0.9439	0.2045	-0.087 $\pm$ i 0.95 -0.040 $\pm$ i 1.87 -0.044	-0.178 $\pm$ i 1.35 +0.020 $\pm$ i 1.87 -0.044
1.241	-0.0404	0.1759	UNSTABLE	UNSTABLE
2.861	-0.0006	0.0139	-0.049 $\pm$ i 1.75 -0.055 $\pm$ i 3.67 -0.088	-0.075 $\pm$ i 1.75 -0.015 $\pm$ i 3.67 -0.177

PARAMETERS: $\dot{\phi}_S = 3.0$, $h = 0.1$, $\phi_M = 90^\circ$, $G = 5.0$, $\sigma = 0.1$.

Parameters $\hat{H}$ and $\hat{K}_p$ were selected for the parametric analysis. $\hat{H}$ represents the damping in yaw of the projectile and $\hat{K}_p$ stands for the roll damping effect. The root locus plot for the eigenvalues of the solution at resonance ($\dot{\phi}_e$=1.011) with variation of parameters $\hat{K}_p$ and $\hat{H}$ is respectively presented in Fig.4.6(a) and Fig.4.6(b). The eigenvalues (poles) of the equilibrium solution at resonance for the base parameter values assumed above are shown by the symbol 'X'. The two pairs of complex poles represent the pitch-yaw motion, while the lone real pole represents the rolling motion. The arrows show the direction in which the poles shift as the parameter value is varied through its base value. Only qualitative shift in the pole location is shown; a longer arrow indicating a larger shift.

As is well known, stability requires all the poles to lie in the left half plane. Fig.4.6 reveals that the complex pair of poles closer to the imaginary axis crosses over to the right half plane with

(i) an increase in the value of $\hat{K}_p$, and

(ii) a decrease in the value of $\hat{H}$.

This results in the equilibrium solutions at resonance becoming unstable.

To illustrate, we consider the following values of the parameters $\hat{H}$ and $\hat{K}_p$ with all the other parameters fixed at the same values assigned to them earlier (Table 4.2):

$$\hat{H} = 0.08, \quad \hat{K}_p = 0.20.$$

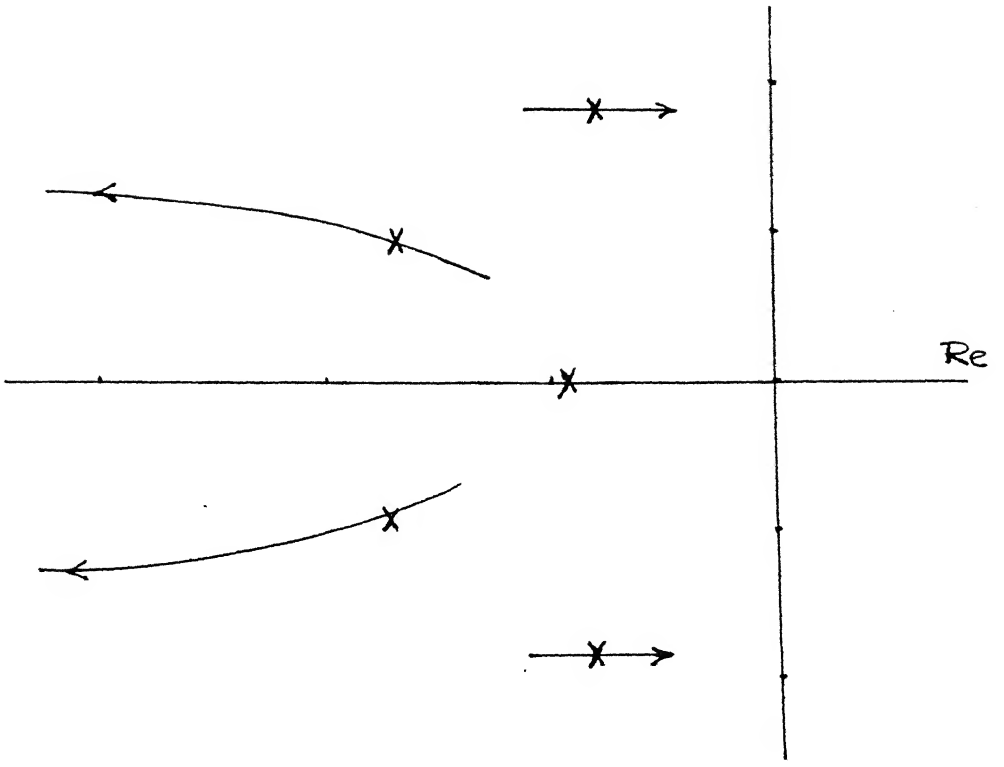

(a) PARAMETER $\hat{K}_p$

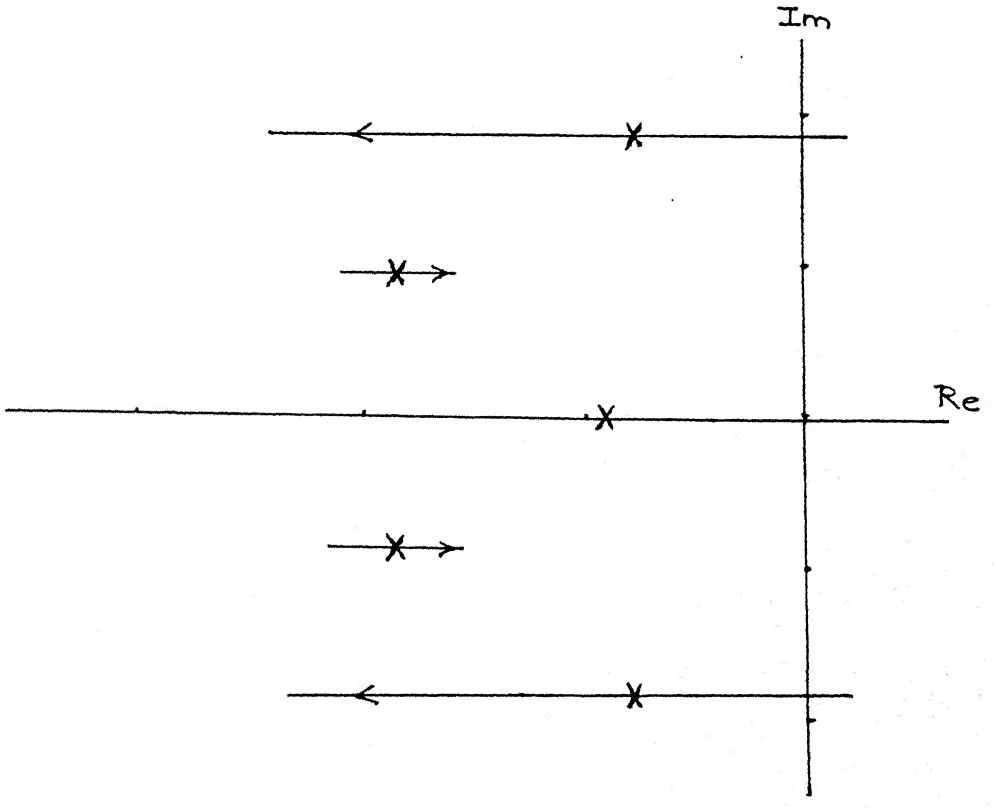

(b) PARAMETER $\hat{H}$

FIG.4.6: ROOT LOCUS OF LOCK-IN SOLUTION

The eigenvalues of the solution at resonance ($\dot{\phi}_e$=1.011) for this set of parameters are also listed in Table 4.2. A pair of complex eigenvalues can be seen to have positive real part indicating instability. On the other hand, the design solution remains stable while the other three unstable solutions given in Table 4.2 were seen to remain unstable for the new parameter values. Thus, the system has only one stable solution, viz. the design solution. Under these circumstances, it seems logical to assume that the projectile will always end up at the design solution for all initial conditions.

To verify this premise, the response from a numerical simulation for this set of parameters is studied and the results are shown in Fig.4.7. Contrary to our expectations, the roll rate can be seen to get locked in at resonance and it then shows small oscillations about the resonance roll rate ($\dot{\phi}$=1). The angle of attack magnitude shows a gradual build-up. Soon, large amplitude yawing motion is seen which lead to instability. This response is typical of catastrophic yaw. It may be noted that in contrast to the bounded oscillations in yaw seen for cases of stable roll resonance (Fig.4.1 and Fig.4.2), the oscillations in Fig.4.7 for an unstable resonance solution are unbounded.

The above analysis reveals two important results.

(i).It is possible to account for the phenomenon of catastrophic yaw without considering the induced side

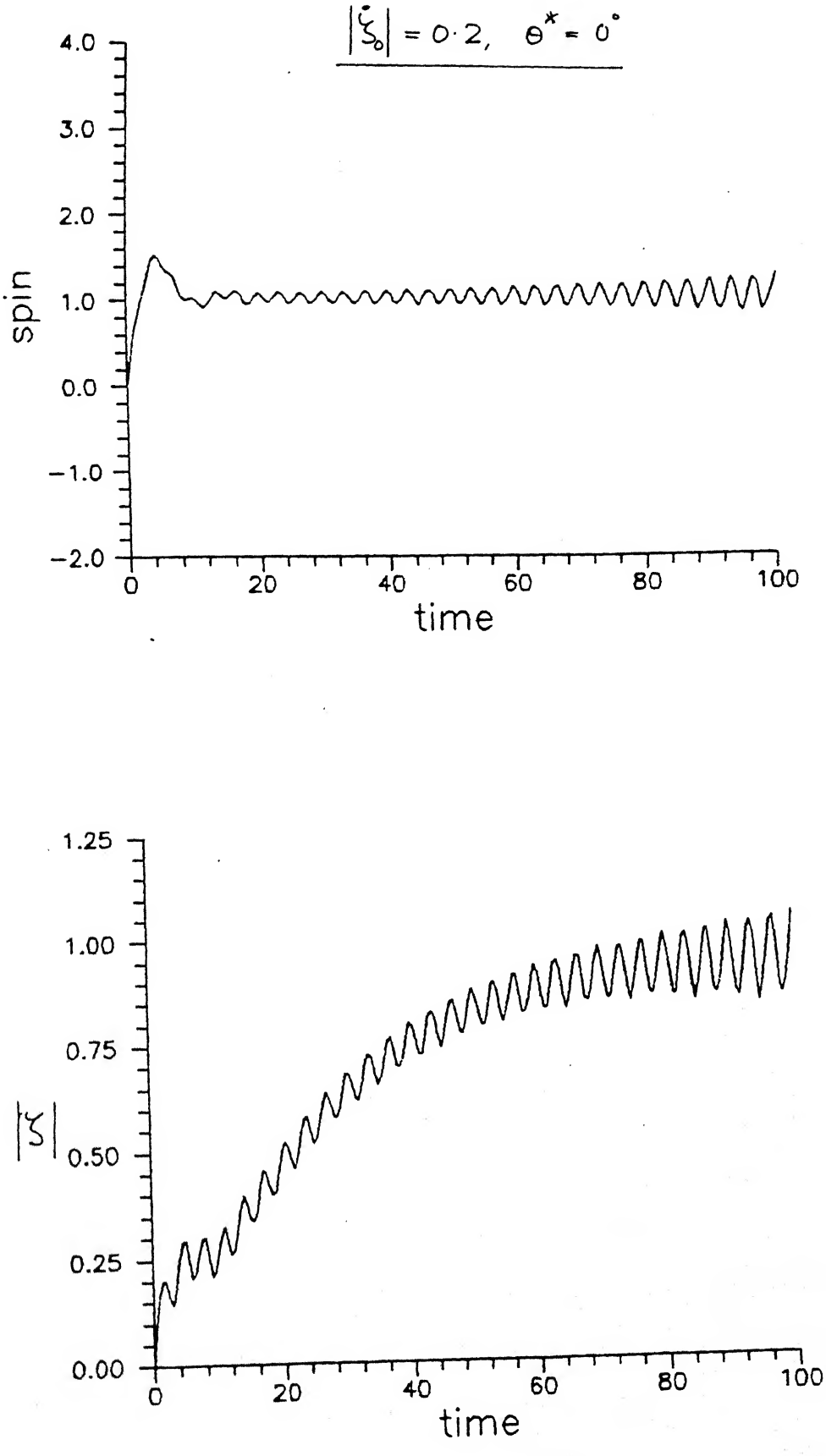

FIG.4.7: CATASTROPHIC YAW

forces and moments in the analysis. This result has not been reported in the literature so far. This may serve to explain many flight failures where the missile unexpectedly destroyed itself after getting locked in at resonance despite being designed to avoid roll resonance.

(ii).An unstable equilibrium solution at resonance does not rule out the occurrence of lock-in. This directly refutes the assertion made by Murphy[19] that unstable equilibrium points have no engineering significance. In fact, an unstable lock-in solution leads directly to catastrophic yaw, whereas for a stable lock-in solution the occurrence of catastrophic yaw needs the presence of induced moments. In that sense, an unstable lock-in solution is potentially more "dangerous".

4.4 Roll Break-Out

From the results of the parametric study in Fig.4.6, the single real root representing the rolling motion does not show any change in its location with variation of the parameters. As such, the occurrence of break-out from lock-in does not seem possible. This was also confirmed by studying the response for varying sets of parameters. However, by including the induced roll moment terms described by Murphy[19] in addition to the rolling moment due to an offset center-of-mass, it may be possible to observe the break-out phenomenon in finned projectiles.

Chapter V

CONCLUSIONS

5.1 Summary and Significance of Results

(a) Resonant lock-in of finned projectiles is seen to occur as a result of aerodynamic and mass asymmetries represented by the parameters h, ϕ_M, and G. These arise from manufacturing and assembly tolerances, fin adjustment, and measurement inaccuracies[10]. It is seen that lock-in solutions are possible only for certain combinations of these parameters. However, these asymmetries are essentially random in nature and the designer has little control over them. He can, at best, ensure stricter control over inaccuracies arising in the production process to minimize the asymmetries. This will, in general, make a lock-in solution less likely.

(b) Between normal and reverse lock-in solutions, it is seen that larger values of mass asymmetry are needed for a reverse solution to exist. This may account for the lack of any reported flight experience of reverse lock-in.

(c) The occurrence of resonant lock-in is largely influenced by the initial conditions at launch. These arise as result of disturbances during the process of firing a projectile and, normally, take the form of a yaw rate.

For parameter combinations that indicate the existence of stable resonant solutions, lock-in for a smaller value of G was seen to require larger initial perturbations. Thus, limiting disturbances at launch in conjunction with small asymmetries could be a possible solution to avoid lock-in.

(d) Sixteen sets of initial conditions were investigated for each of four different parameter combinations to study the influence of the initial conditions on the steady-state response of the projectile. The results revealed that stable lock-in solutions do not occur frequently. It is seen that an unstable solution always exists near every stable resonant (lock-in) solution which effectively limits the number of trajectories of the system leading to the lock-in solution.

(e) The phenomenon of transient resonance is shown where a projectile does not get locked in but stays at resonance for some time as its roll rate builds up to the design value. Our analysis suggests that projectiles experiencing transient resonance show increased damping in their yaw response. This result has not been reported in the literature so far. However, it is felt that the actual behavior of the projectile in flight may be complicated by the presence of nonlinear induced side forces and moments.

(f) The present study reveals the significance of unstable resonance solutions which had been dismissed as unimportant by Murphy[19]. It is seen that an unstable lock-in solution does not rule out the occurrence of roll lock-in.

(g) Further, a projectile which gets locked in at an unstable lock-in solution is seen to exhibit the phenomenon of catastrophic yaw. Thus, our study reveals that the occurrence of catastrophic yaw can be explained without introducing the induced side moments in the analysis.

(h) The phenomenon of roll break-out of finned projectiles cannot be observed on the basis of the present study.

5.2 Recommendations for Further Work

(i) The analysis carried out in the present study can be expanded to incorporate the induced side forces and moments described in the literature[20-22]. Such an extension can be used to investigate the phenomena of transient resonance and catastrophic yaw.

(ii) The possibility of break-out from lock-in of finned projectiles can be studied by including the induced roll moment terms described by Murphy[19] in addition to the rolling moment due to an offset center-of-mass.

LIST OF REFERENCES

1. Fowler,R.H., Gallop,E.G., Lock,C.N.H., and Richmond,H.W., "Aerodynamics of a Spinning Shell," Philosophical Transactions of Royal Society of London (A), Vol.221, 1920, pp.295-387.

2. McShane,E.J., Kelley,J.L., and Reno,F.V., Exterior Ballistics, University of Denver Press, Denver, Colo., 1953.

3. Regan,F.J., Re-Entry Vehicle Dynamics, AIAA Education Series, New York, 1984, pp.235-265.

4. Anon., Textbook of Ballistics and Gunnery, Her Majesty's Stationery Office, U.K.

5. Murphy,C.H., "Symmetric Missile Dynamic Instabilities," Journal of Guidance and Control, Vol.4, No.5, Sept.-Oct.1981, pp.464-471.

6. Platus,D.H., "Ballistic Re-Entry Vehicle Flight Dynamics," Journal of Guidance and Control, Vol.5, No.1, Jan.-Feb.1982, pp.4-16.

7. Nicolaides,J.D., "On the Free Flight Motion of Missiles Having Slight Configurational Asymmetries," IAS Preprint 395, Jan.1953.

8. Murphy,C.H., "The Prediction of Nonlinear Pitching and Yawing Motion of Symmetric Missiles," Journal of Aero Sciences, Vol.24, No.7, July 1957, pp.473-479.

9. Nicolaides,J.D., "Two Nonlinear Problems in the Flight Dynamics of Modern Ballistic Missiles," IAS Report 59-17, Jan.1959.

10. Price,D.A.,Jr., "Sources, Mechanisms, and Control of Roll Resonance Phenomena for Sounding Rockets," Journal of Spacecraft and Rockets, Vol.4, No.11, Nov.1967, pp.1516-1525.

11. Chadwick,W.R., "Flight Dynamics of a Bomb with Cruciform Tail," Journal of Spacecraft and Rockets, Vol.4, No.6, June 1967, pp.768-773.

12. Barbera,F.J., "An Analytical Technique for Studying the Anomalous Roll Behavior of Re-Entry Vehicles," Journal of Spacecraft and Rockets, Vol.6, No.11, Nov.1969, pp.1279-1284.

13. Murphy,C.H., "Nonlinear Motion of a Missile with Slight Configurational Asymmetries," Journal of Spacecraft and Rockets, Vol.8, No.3, March 1971, pp.259-263.

14. Clare,T.A., "On Resonance Instability for Finned Configurations Having Nonlinear Aerodynamic Properties," Journal of Spacecraft and Rockets, Vol.8, No.3, March 1971, pp.278-283.

15. Murphy,C.H., "Response of an Asymmetric Missile to Spin Varying through Resonance," AIAA Journal, Vol.9, No.11, Nov.1971, pp.2197-2201.

16. Nayfeh,A.H., and Saric,W.S., "An Analysis of Asymmetric Rolling Bodies with Nonlinear Aerodynamics," AIAA Journal, Vol.10, No.8, Aug.1972, pp.1004-1011.

17. Kevorkian,J., "On a Model for Re-Entry Roll Resonance," SIAM Journal of Applied Mathematics, Vol.26, No.3, May 1974, pp.638-669.

18. Lewin,L., and Kevorkian,J., "On the Problem of Sustained Resonance," SIAM Journal of Applied Mathematics, Vol.35, No.4, Dec.1978, pp.739-754.

19. Murphy,C.H., "Some Special Cases of Spin-Yaw Lock-In," Journal of Guidance and Control, Vol.12, No.6, Nov.-Dec.1989, pp.771-776.

20. Ling,Y.L., and Han,K.W., "Stability Analysis of Angular Motion of Rolling Missiles," Israel Journal of Technology, Vol.18, 1980, pp.65-69.

21. Pepitone,T.R., and Jacobson,I.D., "Resonant Behavior of a Symmetric Missile Having Roll-Orientation Dependent Aerodynamics," Journal of Guidance and Control, Vol.1, No.5, Sept.-Oct.1978, pp.335-339.

22. Ingram,C.W., and Nicolaides,J.D., "Obtaining Nonlinear Aerodynamic Stability Coefficients from Free Angular Motion of Rigid Bodies," Journal of Spacecraft and Rockets, Vol.8, No.4, April 1971, pp.390-395.

APPENDIX A

Equations (2.1) can be combined to give

$$F_y + iF_z = m\,[\,(\dot{v} + i\dot{w}) - iu(q + ir)\,] \quad ...(A.1)$$

On expressing F_y and F_z in terms of non-dimensional force coefficients

$$C_y + iC_z = (2m/\rho u^2 S)\,[\,\tilde{\xi} - i(q+ir)\,] - C_D\tilde{\xi} \quad ...(A.2)$$

where it is assumed that $V \approx u$.

The linear aerodynamic force for a slightly asymmetric missile can be written as[19]

$$C_y + iC_z = -C_{N_\alpha}\tilde{\xi} - C_{N_0}\exp[i(\Phi + \Phi_N)] \quad ...(A.3)$$

(A.2) and (A.3) can be solved to give the complex angular velocity as

$$q + ir = i(\rho uS/2m)[-C_{L_\alpha}\tilde{\xi} - C_{N_0}\exp[i(\Phi + \Phi_N)] - i\dot{\tilde{\xi}} \quad ...(A.4)$$

Equations (2.3) can be put together as

$$M + iN = I\,(\dot{q} + i\dot{r}) - ipI_x(q + ir) \quad ...(A.5)$$

Using non-dimensional moment coefficients

$$C_m + iC_n = (2I/\rho u^2 Sl)\,[(\dot{q} + i\dot{r}) - ip\bar{D}(q + ir)] \quad ...(A.6)$$

A linear expansion for the aerodynamic moment can be written as[19]

$$C_m + iC_n = [\Phi' C_{M_{P\alpha}} - iC_{M_\alpha}]\tilde{\xi} - i(C_{M_q} + C_{M_{\dot{\alpha}}})\tilde{\xi}' - iC_{M_0}\exp[i(\Phi + \Phi_M)] \quad ...(A.7)$$

where $'$ denotes differentiation with respect to dimensionless time, s.

Using (A.4) and its derivative in (A.6) along with (A.7) gives the linear pitch-yaw equation as[19]

$$\tilde{\xi}'' + (H - i\sigma\Phi')\tilde{\xi}' - (M + i\sigma\Phi' T)\tilde{\xi}$$
$$= -M_A \exp[i(\Phi + \Phi_M)] \qquad \ldots(A.8)$$

where

$$M_A = -(\rho S l^3/2I)\{C_{M_0} - ik_t^2(i-\sigma)\Phi' C_{N_0}\exp[i(\Phi_N - \Phi_M)]\} \qquad \ldots(A.9)$$

Equation (3.3) for the roll moment in conjunction with (2.2) gives

$$L_p p + L_\delta \delta_f + L_\theta(\theta,\delta) = I_x \dot{p} \qquad ..(A.10)$$

Using the expression for L_θ from (3.4), this can be put in the notation of Ref[19] as

$$\Phi'' + K_p[\Phi' - \Phi_s' - iK_\theta(\xi - \bar{\xi})] = 0 \qquad ..(A.11)$$

where ' refers to derivative w.r.t. dimensionless time, s.

Murphy[19] introduces another dimensionless time, τ, where

$$\tau = [-M/(1-\sigma)]^{1/2} s \qquad ..(A.12)$$

The term within the brackets in (A.12) can be seen to be equal to the resonance roll rate given by (2.17). Thus, the effect of the transformation (A.12) is to scale the roll rate in (A.11) by its value at resonance. Now, the roll rate at resonance will be given by $\dot{\Phi}=\pm 1$.

With the simplifications adopted by Ref[19], (A.8) can be transformed to

$$\ddot{\tilde{\xi}} + (\hat{H} - i\sigma\dot{\phi})\dot{\tilde{\xi}} + (1-\sigma-i\sigma\dot{\phi}\hat{T})\tilde{\xi} = \delta_{TO}(1-\sigma)\exp[i(\phi+\phi_M)] \qquad ..(A.13)$$

where '.' denotes derivative w.r.t. the independent variable τ. δ_{TO} in (A.13) stands for the magnitude of the initial trim and σ is the ratio of axial to transverse moment of inertia.

At the steady-state, the nutation and precession modes are assumed[19] to have damped out and the response is taken to consist only of the trim.

$$\tilde{\xi} = \xi_T \exp(i\phi) \qquad ..(A.14)$$

where substituting (A.14) in (A.13) gives

$$\xi_T = \frac{\delta_{TO}\exp(i\phi_M)}{1-\dot{\phi}^2+i\dot{\phi}h} = \delta_T\exp[i(\phi_T+\phi_M)] \qquad ..(A.15)$$

At resonance ($|\dot{\phi}|=1$), the trim angle magnitude can be written from (A.15) as

$$\delta_{TR} = \delta_{TO}/|h| \qquad ..(A.16)$$

Using (A.16), a scaled complex angle of attack can be defined as

$$\zeta = \xi/\delta_{TR} \qquad ..(A.17)$$

(A.11) and (A.13) can be put in the following form using (A.17):

$$\ddot{\phi} + \hat{K}_p[\dot{\phi} - \dot{\phi}_S - iG(\zeta - \bar{\zeta})] = 0 \qquad ..(A.18)$$

$$\ddot{\xi} + [\hat{H} + i(2-\sigma)\dot{\phi}]\dot{\xi} + (1-\sigma)[1-\dot{\phi}^2+i\dot{\phi}h + i\ddot{\phi}]\xi = (1-\sigma)|h|\exp(i\phi_M) \qquad ..(A.19)$$
